Modelling water storage capacity in small, constructed wetlands – today and in the future

Alina Leonie Kuehn

Degree project/Independent project • 30 credits
Swedish University of Agricultural Sciences, SLU
Faculty of Natural Resources and Agricultural Sciences/ Department of Aquatic Sciences and Assessment
EnvEuro - European Master in Environmental Science
Uppsala 2024

Modelling water storage capacity in small, constructed wetlands – today and in the future

Alina Leonie Kuehn

Supervisor:	**Emma Lannergård, Swedish University of Agricultural Sciences, Department of Aquatic Sciences and Assessment**
Assistant supervisor:	Joachim Ingwersen, University of Hohenheim, Institute of Soil Science and Land Evaluation
Examiner:	Martyn Futter, Swedish University of Agricultural Sciences, Department of Aquatic Sciences and Assessment

Credits:	30 credits
Level:	Second-cycle
Course title:	Master thesis in Environmental science
Course code:	A2E – EX0897
Programme/education:	EnvEuro - European Master in Environmental Science
Course coordinating dept:	Department of Aquatic Sciences and Assessment
Place of publication:	Uppsala
Year of publication:	2024

| **Keywords:** | Hydrological modelling, constructed wetlands, water storage capacity, climate change, extreme precipitation |

Swedish University of Agricultural Sciences
Faculty of Natural Resources and Agricultural Sciences
Department of Aquatic Sciences and Assessment
Division of Geochemistry and Hydrology

Abstract

Wetlands, regardless of their size, contribute essentially to ecosystem services and are therefore vital to sustaining human life and the functioning of the environment. At the same time, wetlands are decreasing at an alarming speed and are exposed to considerable threats. Current policies and programs are not able to stop this trend which is amplified by a lack of research. Due to their potential to reduce runoff and prevent flooding, wetlands have recently gained more research attention. This study aims to model and assess the water storage capacity and thus the flood buffering capacity of ten constructed wetlands in Mälardalen, Sweden, under present and potential future climate scenarios. The hydrologic model PERSiST, a semi-distributed rainfall-runoff model, was employed to reproduce water level observations for constructed wetlands with hourly driving data for a 30-year period. Based on a conceptual model depicting water level patterns of all constructed wetlands with the underlying processes and interactions, observed water level data for 2023 was calibrated against hourly air temperature and precipitation ERA5-Land data. Driving data for the baseline scenario was produced with ERA5-Land data from 1971-2000 and was adapted with Regional Climate model data from SMHI to generate RCP4.5 and RCP8.5 scenarios. Extreme precipitation stretch scenarios were employed to model extreme precipitation events. Results for a subset of three ponds for the 12 different climate scenarios showed no indication of drying out nor a major difference between baseline and RCP4.5 and RCP8.5 scenarios. Stretched RCP and extreme precipitation stretch scenarios presented major variations in water level behaviour, especially in summer and fall. Important factors influencing the flood buffering capacity are the relative area of a constructed wetland, their purpose and design as well as interactions with their surrounding environment. The future climate scenarios suggest that current pond design makes constructed wetlands in Mälardalen resilient against an overall increase of temperature and precipitation but needs further research development regarding extreme precipitation events.

Keywords: Hydrological modelling, constructed wetlands, water storage capacity, climate change, extreme precipitation

Table of contents

List of tables **6**

List of figures **7**

Abbreviations **9**

1. Introduction **11**

2. Materials and methods **14**

2.1 Study site 14

2.2 PERSiST 16

2.3 Model input data 16

2.3.1 Meteorological data 16

2.3.2 Hydrological data 17

2.4 Model setup and calibration 17

2.5 Future climate scenarios 20

2.5.1 Baseline scenario 20

2.5.2 RCP scenarios 20

2.5.3 Extreme precipitation stretches 21

2.6 Data analysis 22

2.7 Literature review 22

3. Results **23**

3.1 Water level measurements in 2023 23

3.2 Monte Carlo analysis 27

3.3 Future climate scenarios 27

4. Discussion **35**

4.1 PERSiST feasibility 35

4.2 Developing future climate scenarios 36

4.3 Flood buffering capacity under future climate scenarios 38

4.4 Limitations 40

4.4.1 Calibration period 40

4.4.2 Statistical evaluation 40

4.4.3 Relative water level as proxy for water storage capacity 41

4.4.4 Policy and design recommendations 41

5. Conclusions **42**

References **44**

Popular science summary **50**

Acknowledgements **52**

Appendix **53**

List of tables

Table 1. General, topographical, land cover, soil and hydrological characteristics of the different CWs. “*” indicates the CW’s dominant soil type.” **” indicates postglacial fine clay. 15

Table 2. Square matrix representing water flows in PERSiST. 18

Table 3. Seasonal changes in precipitation [%] and temperature [°C] for RCP4.5 and RCP8.5 in SC, UC and VC for the period 2041-2070 compared to baseline period 1971-2000 (SMHI, 2024). 21

Table 4. Nash-Sutcliffe efficiency for the best and the worst performing parameter set in the ensemble of the ten best performing parameter sets for Aby, Bru and Gra. 27

List of figures

Figure 1. Study area Mälardalen, Sweden. Red points indicating examined constructed wetlands. This map was created by the author using ArcGIS Pro with data from Lantmäteriet and Geological Survey of Sweden. 14

Figure 2. Conceptual model of surface and subsurface interactions for CWs including the components direct runoff, upper soil water, lower soil water, upper groundwater, lower groundwater, riparian unsaturated zone and CW including the processes overland flow, evapotranspiration, precipitation and percolation. 18

Figure 3. Description of which scenarios were used. Boxes show different climate scenarios, arrows show which scenarios were additionally combined. 20

Figure 4. Relative water level data plotted against precipitation data for CW in Västmanland County for the year 2023. Missing values indicate removed outliers. 25

Figure 5. Relative water level data plotted against precipitation data for CW in Uppsala County for the year 2023. Missing values indicate removed outliers. 26

Figure 6. Relative water level data plotted against precipitation data for CW in Stockholm County for the year 2023. Missing values indicate removed outliers. 26

Figure 7. Projected mean water level [m] for Aby for the baseline scenario and the different future climate scenarios for the period 2041-2070. 28

Figure 8. a) Minimum relative water level of ensemble data grouped by season (winter, spring, summer, fall) for Aby for the period 2041-2070. b) Mean relative water level of ensemble data grouped by season (winter, spring, summer, fall) for Aby for the period 2041-2070. c)Maximum relative water level of ensemble data grouped by season (winter, spring, summer, fall) for Aby for the period 2041-2070. 29

Figure 9. Projected mean water level [m] for Bru for the baseline scenario and the different future climate scenarios for the period 2041-2070. 30

Figure 10. a) Minimum relative water level of ensemble data grouped by season (winter, spring, summer, fall) for Bru for the period 2041-2070. b) Mean relative water level of ensemble data grouped by season (winter, spring, summer, fall) for Bru

for the period 2041-2070. c)Maximum relative water level of ensemble data grouped by season (winter, spring, summer, fall) for Bru for the period 2041-2070. 31

Figure 11. Projected mean water level [m] for Gra for the baseline scenario and the different future climate scenarios for the period 2041-2070. 32

Figure 12. a) Minimum relative water level of ensemble data grouped by season (winter, spring, summer, fall) for Gra for the period 2041-2070. b) Mean relative water level of ensemble data grouped by season (winter, spring, summer, fall) for Gra for the period 2041-2070. c)Maximum relative water level of ensemble data grouped by season (winter, spring, summer, fall) for Gra for the period 2041-2070. 33

Abbreviations

Aby	Åby
Bru	Brunnby
CORDEX	Coordinated Regional Downscaling Experiment
CW	Constructed wetland
DR	direct runoff
ECMWF	European Centre for Medium-Range Weather Forecasts
ERA5-Land	5th generation of European ReAnalysis dataset
EU	European Union
fall	September-November
GIS	Geographical Information System
Gra	Graneberg
IPCC	Intergovernmental Panel on Climate Change
KLu	Kanik-Lundby
Kur	Kurö
LGW	lower groundwater
LiDAR	High-resolution, airborne light detection and ranging data
LSW	lower soil water
MC	Monte Carlo
NSE	Nash-Sutcliffe efficiency
Pad	Paddeborg
PERSiST	Precipitation, Evaporation and Runoff Simulator for Solute Transport model
RCM	Regional Climate Model
RCP	Representative Concentration Pathway
RipUS	riparian unsaturated zone
SAl	Stora Alby
SC	Stockholm County
SGU	Geological Survey of Sweden
Ska	Skämstad
Sky	Skystad
SLU	Swedish University of Agriculture
SMHI	Swedish Meteorological and Hydrological Institute
spring	March-May
Stretch2	baseline scenario stretched by 200%
Stretch3	baseline scenario stretched by 300%
Stretch4	baseline scenario stretched by 400%
summer	June-August
UC	Uppsala County

UERRA	Uncertainties in Ensembles of Regional Reanalysis
UGW	upper groundwater
USW	upper soil water
VC	Västmanland County
WFD	Water Framework Directive 2000/60/EC
Wig	Wiggeby
winter	December-February

1. Introduction

Wetlands, regardless of their size, contribute essentially to environmental, social and economic ecosystem services and are therefore vital to sustaining human life and the functioning of the environment (Graversgaard *et al.*, 2021; Hambäck *et al.*, 2023). Even though they only cover 6 % of terrestrial area globally, the estimated value of wetland services is approximately €24.6 trillion (~ $26.4 trillion) per year (Thorslund *et al.*, 2017). According to Costanza *et al.* (2014) inland wetlands have the second highest value as providers of ecosystem services with only the entire entity of coastal biomes being higher.

At the same time, wetlands are exposed to considerable threats caused by a growing population and its associated consequences, such as land use change and agricultural intensification (Graversgaard *et al.*, 2021; Hill *et al.*, 2021). To prevent deterioration and reduce possible threats to all surface water bodies the EU implemented the Water Framework Directive 2000/60/EC (WFD; European Commission, 2000), though a large fraction of wetlands is neglected as the WFD leaves out water bodies smaller than 50 ha.

Reportedly, Sweden has already lost an average of 65 % of its wetlands and up to 90 % in specific areas (European Commission, 2007; Jonstrup, 2024). National regulations on wetland restoration and protection were adapted in Sweden long before the European Union issued the WFD or other directives to guard water bodies from potential threats. These policies have led to 7.800 ha of newly constructed wetlands (CW) between 1990-2010 (Strand and Weisner, 2013).

In Sweden an CW can generally be defined as newly created permanent or temporal surface water body raising the water table or lowering the ground level or most commonly a combination of both (Lutton, Sheldon and Bunn, 2010; Strand and Weisner, 2013). Even though the trend is still increasing, objectives like in the "thriving wetland" program are regularly not met (Graversgaard *et al.*, 2021; Åhlén *et al.*, 2022).

Additional to the lack and inefficiency of legislative protection, large gaps in research and understanding of underlaying processes exist (Hill *et al.*, 2021;

Nakashima *et al.*, 2024). Hydrologic connectivity of wetlands and their surroundings and the resulting effects on biotic and abiotic factors can already vary for wetlands with similar characteristics and topography and are even more distinct with higher diversity (Golden *et al.*, 2014; Ameli and Creed, 2017; McLaughlin *et al.*, 2019).

Wetland water level patterns and their storage capacity is one important parameter that has received too little attention in research so far and even less in northern European countries controlled by long winters and snowmelt processes (Karimi, Seibert and Laudon, 2022; Åhlén *et al.*, 2022).

Water storage capacity provides not only useful insight on the well-being of a wetland but contributes strongly to ecosystem services at the same time. Recent papers (Kadykalo and Findlay, 2016; Thorslund *et al.*, 2017; Åhlén *et al.*, 2022; Hambäck *et al.*, 2023) emphasize that wetlands can potentially serve to reduce runoff and prevent flooding.

Since wetlands react sensitively to hydro-climatic alterations, which can be amplified by other simultaneously occurring factors, it is essential to gain more knowledge and understanding of water storage and underlying processes to successfully prevent wetland deterioration with smart and pro-active regulations and comprehensive design (Cui *et al.*, 2021; Åhlén *et al.*, 2021).

Climate change will alter the hydrological cycle irreversibly and therefore, needs to be taken into consideration as an additional serious threat. The latest Intergovernmental Panel on Climate Change (IPCC) assessment has shown high confidence in increased observed and projected mean temperature and heavy precipitation in Northern Europe. Additionally, maximum one day precipitation is estimated to intensify by at least 5 % up to over 10 % in all of Sweden in a scenario with a temperature increase of 3 °C, all this leading to changes in the hydro-climatic environment (SMHI, 2019; IPCC, 2021, 2022).

Projecting climate change scenarios has moved more into focus in recent years because it is necessary to estimate and analyze the significance of their effects on the environment and human-beings. Therefore projections have improved largely by downscaling Regional Climate Models (RCM) to a higher spatial and temporal resolution and by creating larger ensembles like the Coordinated Regional Downscaling Experiment (CORDEX) as part of the World Climate Research Programme (Coppola *et al.*, 2021; Vautard *et al.*, 2021).
Still, major obstacles persist, like systematic biases and differences between Global Climate Models and RCMs, which greatly influence the results, especially

regarding extreme precipitation projections. Also, practical issues like the need for high computational power and storage capacities for simulations complicate matters (Sunyer *et al.*, 2015; Jacob *et al.*, 2020; Coppola *et al.*, 2021).

Models allow to imply all these factors and reproduce hydrological connectivity behaviour and water storage patterns under present but also potential future climate scenarios. Although modelling efforts have been made on different spatial and temporal scales to assess these questions, different constraints and limitations hinder applicability to a wider range of wetlands (Ali *et al.*, 2015; Evenson *et al.*, 2016; Ameli and Creed, 2017; Jones *et al.*, 2019; Papa and Frappart, 2021).

The Precipitation, Evaporation and Runoff Simulator for Solute Transport (PERSiST) hydrological model is a semi-distributed rainfall-runoff model with a bucket-type structure at watershed scale. It is designed to reproduce streamflow and runoff patterns (Futter *et al.*, 2014). Due to its ability to be calibrated against water level, the flexible design of various processes and the user-friendliness it was chosen for this study.

This study aims to model the water storage capacity of ten small CWs in Mälardalen under changing climate conditions using high-resolution temporal data, therefore:

(a) A representative conceptual model is designed to describe the water level patterns of all ten CWs, which is then used as a base for a multi-setup-approach in PERSiST, a simple semi-distributed rainfall-runoff model.
(b) A baseline scenario, different Representative Concentration Pathways (RCP), namely RCP4.5 and RCP8.5, as well as different extreme precipitation stretch scenarios are developed and compared. All scenarios consist of hourly data for a period of 30 years (2041-2070).
(c) Feasibility of PERSiST to model water level changes and results of the assessment between the baseline scenario and the different potential future scenarios are examined for flood buffering capacity.

2. Materials and methods

2.1 Study site

Ten construced wetlands in the greater Mälardalen area in Central Sweden were examined (figure 1).

Though geographically distributed over Västmanland County (VC), Uppsala County (UC) and Stockholm County (SC) all ponds lay within the warm temperate region without a dry season and a warm summer according to the re-analyzed Köppen-Geiger Classification (Rubel *et al.*, 2017).

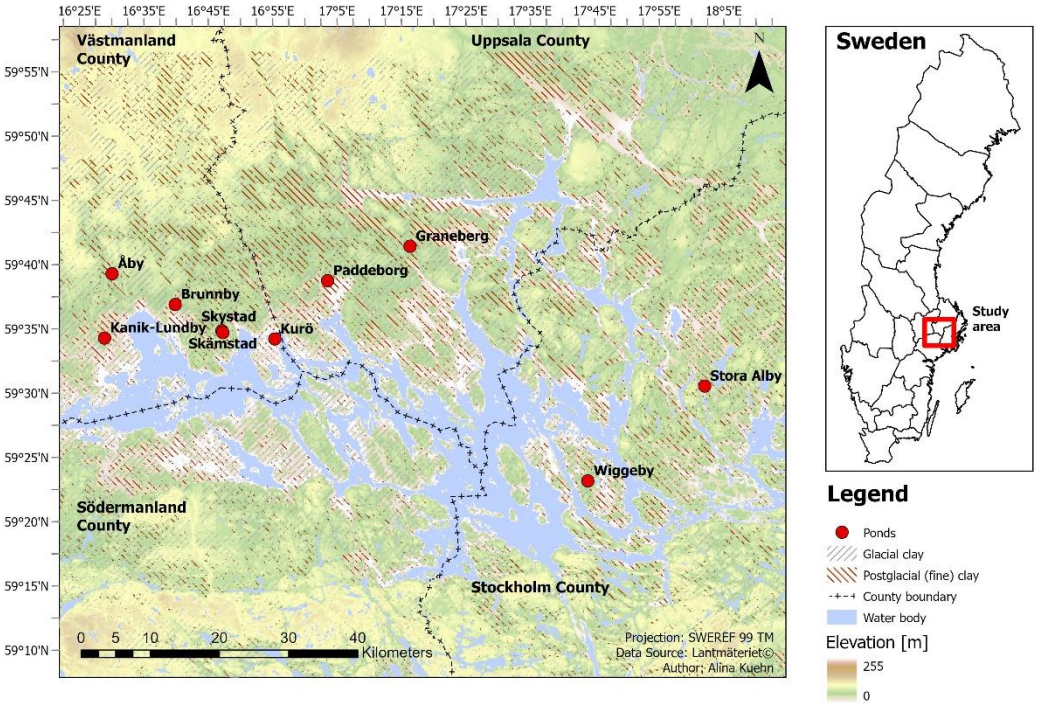

Figure 1. Study area Mälardalen, Sweden. Red points indicating examined constructed wetlands. This map was created by the author using ArcGIS Pro with data from Lantmäteriet and Geological Survey of Sweden.

Mean annual temperature for the period 1981-2010 was 5.9 °C with a mean annual precipitation of 633.2 mm in VC and respectively 5.9 °C and 596.8 mm in UC and 6.4 °C and 585.2 mm in SC (SMHI, 2024).
The main land cover classes in this lowland area are forest, agriculture and other open land on predominantly glacial and postglacial (fine) clay soils.

To determine hydrological and morphological characteristics of each CW Geographical Information System (GIS) mapping was employed. Analyses were performed with ArcGIS Pro (Version 3.3.0, ESRI, 2024) using maps and geodata provided by Lantmäteriet and the Geological Survey of Sweden (SGU). Data was obtained on land cover classes (GSD-Topographic Map 1:50 000, Lantmäteriet), elevation (GSD-Elevation data, grid 50+, Lantmäteriet), soil types (Soil Type Map 1:25 000-1:100 000, SGU) and distance to groundwater magazines (Groundwater 1:1 million, SGU) for the ponds' catchment areas. Additional information was collected by site visits. A detailed description of the wetlands' properties can be found in table 1.

Table 1. General, topographical, land cover, soil and hydrological characteristics of the different CWs. "" indicates the CW's dominant soil type." **" indicates postglacial fine clay.*

Properties	**Unit**	**Åby** (Aby)	**Brunnby** (Bru)	**Graneberg** (Gra)	**Kanik-Lundby** (Klu)	**Kurö** (Kur)	**Paddeborg** (Pad)	**Skystad** (Sky)	**Skämstad** (Ska)	**Stora Alby** (Sal)	**Wiggeby** (Wig)
GENERAL											
Latitude (N)		59.653	59.612	59.678	59.570	59.563	59.637	59.576	59.573	59.482	59.366
Longitude (E)		16.487	16.647	17.253	16.463	16.898	17.038	16.764	16.766	17.991	17.684
Type of pond		P-retention	P-retention	Biodiversity	P-retention	Biodiversity	P-retention	P-retention	P-retention	P-retention	P-retention
Inlet		Open ditch	Drainage pipe	Drainage pipe	Drainage pipe	2 Pipes	Open ditch	Pipe	Pipe	Pipe	Pipe
Outlet		Open ditch with V-notch	Horizontal drainage pipe	Drainage pipe	Drainage pipe	Drainage pipe	Open ditch	Open ditch	Open ditch	Pipe	Open ditch with V-notch
Deepest point	[m]	1.4	1	0.6	1	0.4	0.9	0.8	1.5	1	1
Length	[m]	140	167	209	51	220	175	21	56	64	90
Width	[m]	15	11	67.5	12	54	11.5	7	6	8	7
TOPOGRAPHY											
Catchment area	[km²]	2.33	1.2	0.25	0.58	1.32	1.71	0.2	0.52	0.32	1.45
Elevation range	[m]	10 to 59	9 to 32	17 to 28	13 to 32	0 to 24	4 to 37	16 to 39	14 to 45	7 to 31	1 to 43
Wetland area	[km²]	0.001608	0.001475	0.013101	0.000567	0.011112	0.0018205	0.000128	0.000336	0.000495	0.0005881
Relative area	[%]	0.07	0.12	5.24	0.10	0.84	0.11	0.064	0.06	0.16	0.04
LAND COVER											
Forest	[%]	47	8	11	35	10	41	46	37	48	52
Agriculture	[%]	52	84	68	54	38	48	33	55	15	36
Other open land	[%]	1	8	21	11	52	11	21	8	37	12
SOIL											
Bedrock	[%]	9	3	3	16	13	5	12	6	15	29
Glacial clay	[%]	47	38	26	49	48	28	37	32	22	58*
Postglacial (fine) clay	[%]	19*	51*	47*/**	18*	22*	34*	18*	33*	34*	6
Sandy moraine	[%]	23	6	14	18	16	33	33	29	29	7
HYDROLOGY											
Closest groundwater magazine	[km]	5-10	< 1	< 1	5-10	1-5	1-5	1-5	1-5	1-5	1-5

2.2 PERSiST

PERSiST is a semi-distributed rainfall-runoff model at watershed scale. Its process-based bucket-type structure allows to assess and model quantitative hydrological patterns such as runoff or streamflow requiring time series of observed or downscaled model data on air temperature and precipitation (Futter et al., 2014).

Therefore, a landscape (level 1) is made up of one or more sub catchments/ reaches (level 2), which consist of different hydrologic response units (level 3) being combined out of different buckets (level 4). Users can apply a wide variety of different scenarios by adapting the levels and how water is routed through them and hence reproduce processes and relationships according to their needs. Processes are reproduced as a set of first-difference equations. A comprehensive description of PERSiST can be found in Futter et al. (2014).

Unlike previous studies with PERSiST (Salmonsson, 2013; Futter *et al.*, 2014, 2015; Deutscher, Hemr and Kupec, 2021; Laguna Marín, 2022), which focused on simulating either streamflow or runoff patterns with daily time series of air temperature and precipitation and calibrating against runoff, this study used (1) hourly data and (2) was calibrated to water depth in PERSiST 2.0 (Ledesma and Futter, 2020).

2.3 Model input data

As driving data PERSiST needs a time series of precipitation and air temperature data. Additionally, a time series of observed data is necessary for calibration and validation.

2.3.1 Meteorological data

Hourly precipitation and air temperature data was acquired from the freely accessible fifth generation of the European ReAnalysis dataset (ERA5-Land) produced by the European Centre for Medium-Range Weather Forecasts (ECMWF) covering a period from January 1950 until the present with a spatial resolution of 0.1° x 0.1° and a native resolution of 9 km (Muñoz-Sabater *et al.*, 2021). Data was downloaded from the Copernicus Climate Data Store (https://cds.climate.copernicus.eu). This was used since gridded data has been showing good compatibility with models (Ledesma and Futter, 2017).

Climate data for 2023 was extracted with Panoply (Version 5.3.2 Build PANQ1XN5, NASA/GISS) with a 0.25° latitude x 0.25° longitude resolution for

each county. This is translated into a grid cell size of approximately 27.83 km by 14.33 km in Sweden. For each county a different grid cell was used with the centre at 59.53°N; 16.44°E for VC, 59.53°N; 17.19°E for UC and 59.53°N; 17.69°E.

2.3.2 Hydrological data

Hourly water level measurements were recorded using WT-HR three channel high resolution water level and temperature TrueTrecks (Intech Instruments, no date) from January 1st, 2023, 00:00:00 am till December 31st, 2023, 23:00:00 pm. An exception is Paddeborg, there water level monitoring started May 23rd, 2023, 12:00:00 pm. A data logger was installed at the deepest point of each pond based on bathymetry measurements (Lindau, 2021).
Excel® (Version 2404 Build 16.0.17531.20152, Microsoft® Excel® for Microsoft 365 MSO) was used to prepare the raw data for further analysis. Water levels of the CWs were re-scaled by setting the lowest observed level to one (relative water level) for comparison of water depth dynamics and utilized for further analysis and modelling.
In a next step, RStudio (Version 2023.12.1+402, Posit Software, PBC) was employed to visualize water level and precipitation data for each county separately on one graph (figures 3-5). Water level series were examined for apparent outliers, which were then removed. These could, e.g., be due to values below zero, a sudden and unrelated punctual drop in water level or incorrect measurements. Removed outliers are shown as blank spaces. CWs presenting water level dynamics unrelated to precipitation patterns were excluded from further analysis, as equipment malfunction was suspected. Reasons for exclusion could be either an increase in water level without reported precipitation or a decrease despite reported precipitation.

2.4 Model setup and calibration

Model setup and calibration was carried out in the following steps:

1. A conceptual model for the hydrological response units was developed with the guiding principles to be applicable to all ponds and to depict the surface and subsurface processes of the ponds as close as possible to reality.

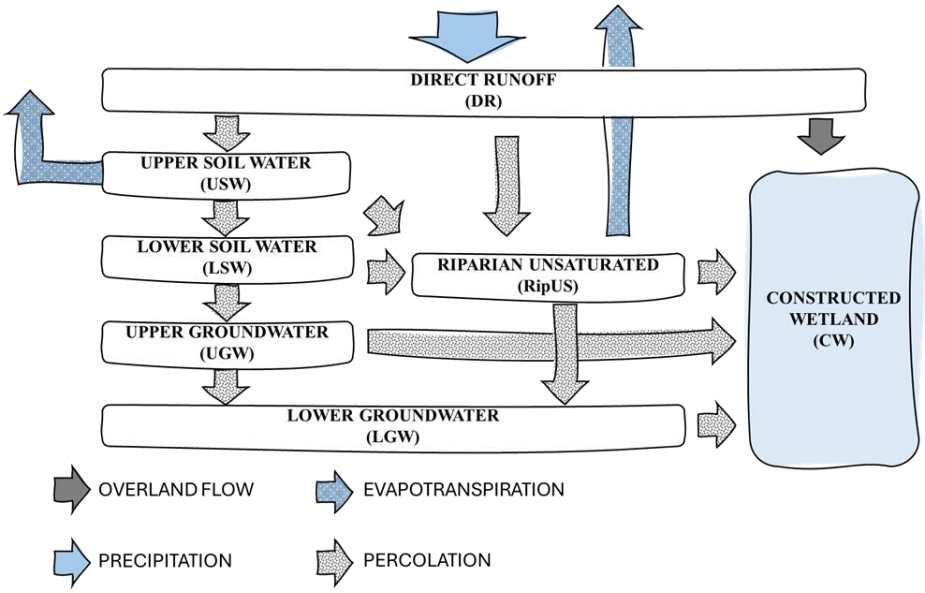

Figure 2. Conceptual model of surface and subsurface interactions for CWs including the components direct runoff, upper soil water, lower soil water, upper groundwater, lower groundwater, riparian unsaturated zone and CW including the processes overland flow, evapotranspiration, precipitation and percolation.

2. The resulting model (figure 2) was then translated into a square matrix used in PERSiST to represent the different buckets and water flows (table 2). Values consist of the two indicators row and column resembling the rows and columns in the matrix, respectively, showing where water can route. Values $v_{row,column}$ need to be chosen between zero and one, they correspond to the water volume in percentage received by a bucket or leaves to the stream. Horizontal values indicate water movement between buckets, the sum of each horizontal row needs to add up to one. Values on the main diagonal represent runoff from the respective bucket to the CW.

Table 2. Square matrix representing water flows in PERSiST.

	Direct runoff	**Upper soil water**	**Lower soil water**	**Upper groundwater**	**Riparian unsaturated**	**Lower groundwater**
Direct runoff	$v_{1,1}$	$v_{1,2}$	$v_{1,3}$	$v_{1,4}$	$v_{1,5}$	$v_{1,6}$
Upper soil water	$v_{2,1}$	$v_{2,2}$	$v_{2,3}$	$v_{2,4}$	$v_{2,5}$	$v_{2,6}$
Lower soil water	$v_{3,1}$	$v_{3,2}$	$v_{3,3}$	$v_{3,4}$	$v_{3,5}$	$v_{3,6}$
Upper groundwater	$v_{4,1}$	$v_{4,2}$	$v_{4,3}$	$v_{4,4}$	$v_{4,5}$	$v_{4,6}$
Riparian Unsaturated	$v_{5,1}$	$v_{5,2}$	$v_{5,3}$	$v_{5,4}$	$v_{5,5}$	$v_{5,6}$
Lower groundwater	$v_{6,1}$	$v_{6,2}$	$v_{6,3}$	$v_{6,4}$	$v_{6,5}$	$v_{6,6}$

This setup comprises important landscape features , creating a more realistic model image. At the same time, it allows to not route water through buckets that are not needed in certain CW.

3. Based on this square matrix an initial manual calibration against observed water depth in 2023 was performed to reproduce the observed temporal patterns as accurately as possible. Due to the small catchment sizes of the wetlands only one reach was used for each model and two land cover classes were used for simplicity. Individual quantitative parameters for each pond were retrieved from previous GIS analyses and did not vary. The following parameters were altered and explored within the ranges stated in Futter *et al.*, (2014) and Ledesma and Futter (2020): threshold temperatures for rain/snow and onset of transpiration, relative amounts of water moving between boxes, boxes characteristic time constants, parameters controlling evaporation rates, parameters for estimating stream depth, Manning's roughness, parameters describing initial and retained water depth as well as infiltration.

4. Nash-Sutcliffe efficiency (NSE; Nash and Sutcliffe, 1970) is commonly used to assess goodness-of-fit of hydrological model calibration and performance. The closer NSE is to one the closer the model accuracy (Moriasi *et al.*, 2015; Lamontagne, Barber and Vogel, 2020; Althoff and Rodrigues, 2021). When both a NSE > 0.1 and an additional visual inspection indicated a credible first calibration, a set of plausible parameter ranges was determined.

5. A Monte Carlo (MC) analysis was executed using the set of plausible parameter ranges and following protocols explained in Futter *et al.* (2014). An ensemble of 50 parameter sets with 500 runs for identification of each candidate parameter set allowing five unsuccessful jumps was produced.
6.
7. Parameters, identified as sensitive in a Kolmogorov-Smirnov *d* statistic ($d \geq 0.2$), were adjusted and employed as new set of plausible parameter ranges.

8. Steps five and six were repeated three times. The ten best performing parameters sets based on NSE, of the last MC analysis were chosen as ensemble to model future climate scenarios.

2.5 Future climate scenarios

The ensembles of best performing parameter sets for Åby, Brunnby and Graneberg were used to model behaviour and patterns under different future climate scenarios from 2041 to 2070. Results were compared to a baseline period from 1971-2000. Future climate scenarios can be divided into several and extreme precipitation stretch scenarios. A total of 12 scenarios were generated for each pond (figure 3).

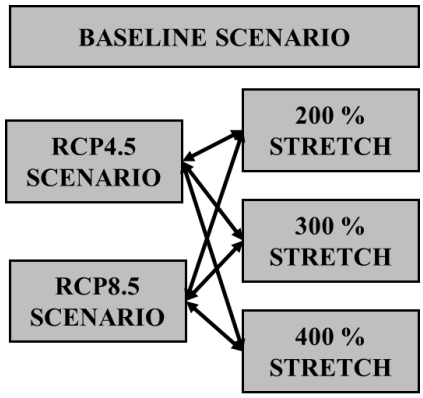

Figure 3. Description of which scenarios were used. Boxes show different climate scenarios, arrows show which scenarios were additionally combined.

2.5.1 Baseline scenario

Hourly precipitation and air temperature data was extracted with Panoply from ERA5-Land data with the same resolution and grid cell centre locations as the meteorological data (2.4.1) for the period 1971-2000. This is coherent with SMHI's reference period (SMHI, 2024).

2.5.2 RCP scenarios

RCP scenarios describe one out of many possible scenarios leading to a certain radiative forcing and hence to a global warming between 2 °C and 4°C by the end of 2100 (IPCC, 2022).

For this study, RCP4.5 and RCP8.5 scenarios were investigated, which limit radiative force at approximately 4.5 W m^{-2} (limit warming to 3 °C) and surpass 8.5 W m^{-2} (exceed warming of 4 °C) in 2100 respectively (IPCC, 2022, 2023).

RCP scenarios were obtained by adapting the baseline scenario with data from the SMHI Advanced Climate Change Scenario Service (SMHI, 2024). Observed data is a combination of Uncertainties in Ensembles of Regional Reanalysis (UERRA; Lopez, 2019) data and actual observations with a high spatial resolution (2.5 x 2.5 km) across Scandinavia for the period 1961-2018. Future changes until 2100 are based on ensembles of downscaled RCMs with a resolution of 12.5 km. Data was bias adjusted with MiltI-scale bias AdjuStment method, and robustness of data was measured in the relative number of models increasing and the standard deviation (SMHI, 2023).

Data is available for each Swedish county for different climate indicators, emission scenarios and the seasons December-February (winter), March-May (spring), June-August (summer) and September-November (fall) (SMHI, 2024). Climate indicators temperature and precipitation were used to calculate changes in temperature and precipitation for RCP4.5 and RCP8.5 scenarios for 2041-2071 (table 3), which were then employed to modify the baseline scenario.

Table 3. Seasonal changes in precipitation [%] and temperature [°C] for RCP4.5 and RCP8.5 in SC, UC and VC for the period 2041-2070 compared to baseline period 1971-2000 (SMHI, 2024).

	SEASON	**RCP4.5**		**RCP8.5**	
		Precipitation [%]	Temperature [°C]	Precipitation [%]	Temperature [°C]
Stockholm county	Winter	+1.17	+3.2	+1.2	+3.6
	Spring	+1.24	+2.6	+1.29	+2.94
	Summer	+1.07	+2.49	+1.08	+3.02
	Fall	+1.09	+2.05	+1.07	+2.76
Uppsala county	Winter	+1.17	+3.32	+1.21	+3.74
	Spring	+1.26	+2.52	+1.32	+2.87
	Summer	+1.1	+2.2	+1.1	+2.71
	Fall	+1.08	+2.01	+1.09	+2.69
Västmanland county	Winter	+1.15	+3.2	+1.19	+3.65
	Spring	+1.28	+2.39	+1.32	+2.72
	Summer	+1.07	+2.05	+1.07	+2.62
	Fall	+1.05	+1.96	+1.07	+2.64

From the projections, hourly precipitation and air temperature data were extracted and used as driving data in PERSiST to model RCP4.5 and RCP8.5.

2.5.3 Extreme precipitation stretches

Future projections of daily (Chen *et al.*, 2015; Rajczak and Schär, 2017; SMHI, 2019) and hourly driven data (Olsson *et al.*, 2013; Olsson and Foster, 2014) agree on an increase of precipitation in frequency as well as intensity till 2100. To capture these extreme events in PERSiST, the reference period was altered using three different extreme precipitation stretch scenarios. This method of generating was introduced by a previous master thesis at SLU (Laguna Marín, 2022).

Analogously to Crespi *et al.* (2020), extreme precipitation hours were defined as hours with an amount of precipitation larger than the 95th percentile. The total amount of precipitation for all days was not changed, but extreme precipitation hours were increased with a constant percentage. The resulting increase corresponds to the amount of precipitation that was subtracted from the hours that were not identified as extreme precipitation hours. Extreme precipitation hours with an already high amount of precipitation were stretched more compared to extreme precipitation hours close to the 95th percentile. Similarly, the amount of

precipitation of hours with already little precipitation becomes even smaller as to the hours close to the 95th percentile (Laguna Marín, 2022).

Results of the stretches were compared with historical SMHI data of extreme precipitation events in Sweden to assess their reasonability and were consistent (SMHI, 2022).

The baseline scenario was then stretched by 200 (Stretch2), 300 (Stretch3) and 400 % (Stretch4 to create scenarios including extreme events.

2.6 Data analysis

Model outputs for relative water level for an ensemble of the ten best performing parametersets according to the NSE of each pond with an hourly timestep for the period 2041-2070 for the baseline and the different future climate scenarios were obtained from PERSiST in Excel. Minimum, mean and maximum relative water level for each ensemble and scenario were calculated in Excel.
Relative mean water level was calculated for each ensemble and each scenario. Using RStudio the results were visualized, and all plotted in one plot.
Additionally, RStudio was employed to create boxplots of minimum, mean and maximum water levels for each ensemble and each scenario across winter, spring, summer and fall.

2.7 Literature review

A literature review of published scientific literature was conducted to find out about the current state of research water level modelling for CWs and compare the results of other studies with the findings in this study. Google Scholar (scholar.google.com, last accessed June 2024) and ScienceDirect (sciencedirect.com, last accessed June 2024). The survey included the keywords “artificial wetlands”, “PERSiST”, “ecological engineering”, “RCPs”, “flood regulation”, “nature-based solutions", “water storage wetlands", “water level dynamics”, “hydroclimatic change” among others.

3. Results

3.1 Water level measurements in 2023

Precipitation pattern in all three counties behaves similarly. Winter month and the first part of spring are dominated by smaller but regular occurring precipitation. From April to July only occasional minor precipitation events can be observed, whereas July to October is characterized by a lot of strong precipitation events. Which decrease again in the rest of fall.

For VC Aby, Sky and Ska show an equal behaviour (figure 4). In periods with less rain relative water level decreases, in case of strong precipitation events a pronounced response mirroring the event can be seen. Water level measurements of Klu showed obvious error in measurements therefore these values were removed. Still Klu relative water level behaves equally like Aby, Sky and Ska.

Bru's response to heavy precipitation is equally pronounced as the other ponds, though it's behaviour throughout the year differs in the dry periods. Relative water level does not decrease but continues to be stable around the same height at approx. 0.12 m. Relative water level pattern observed in Kur does not relate at all with precipitation patterns.

In UC Gra and Pad show a pattern of drying out and regeneration phases, though their response to a lot of precipitation is less pronounced and a lot slower (figure 5). This leads to another slight drying out phase in fall. Only the later precipitation events in fall can increase the relative water level which stabilizes around 0.25 m in winter. Amplitude between peaks and lows is as a result smaller compared to the ponds in VC.

In SC relative water level in Sal appear to be spikier and therefore react more direct to precipitation events (figure 6). Also, the regeneration phase after a drying out phase in summer is shorter compared to the ponds in UC.

Wiggeby's behaviour of relative water level is not corresponding to the precipitation pattern in SC. In summer relative water level increases although only little precipitation can be detected. Around the beginning of August, the pattern shows a regular decrease followed by a strong increase which lasts until the end of the year but does not relate to the precipitation. As a result, the wetlands Wiggeby and Kurö were excluded after visual inspection.

Focus is put on the results of a subset of three ponds with different characteristics in the rest of this study.
Aby a phosphorus-retention pond setup in a stream, Bru a conventional phosphorus-retention pond and Gra, a pond designed to increase biodiversity.

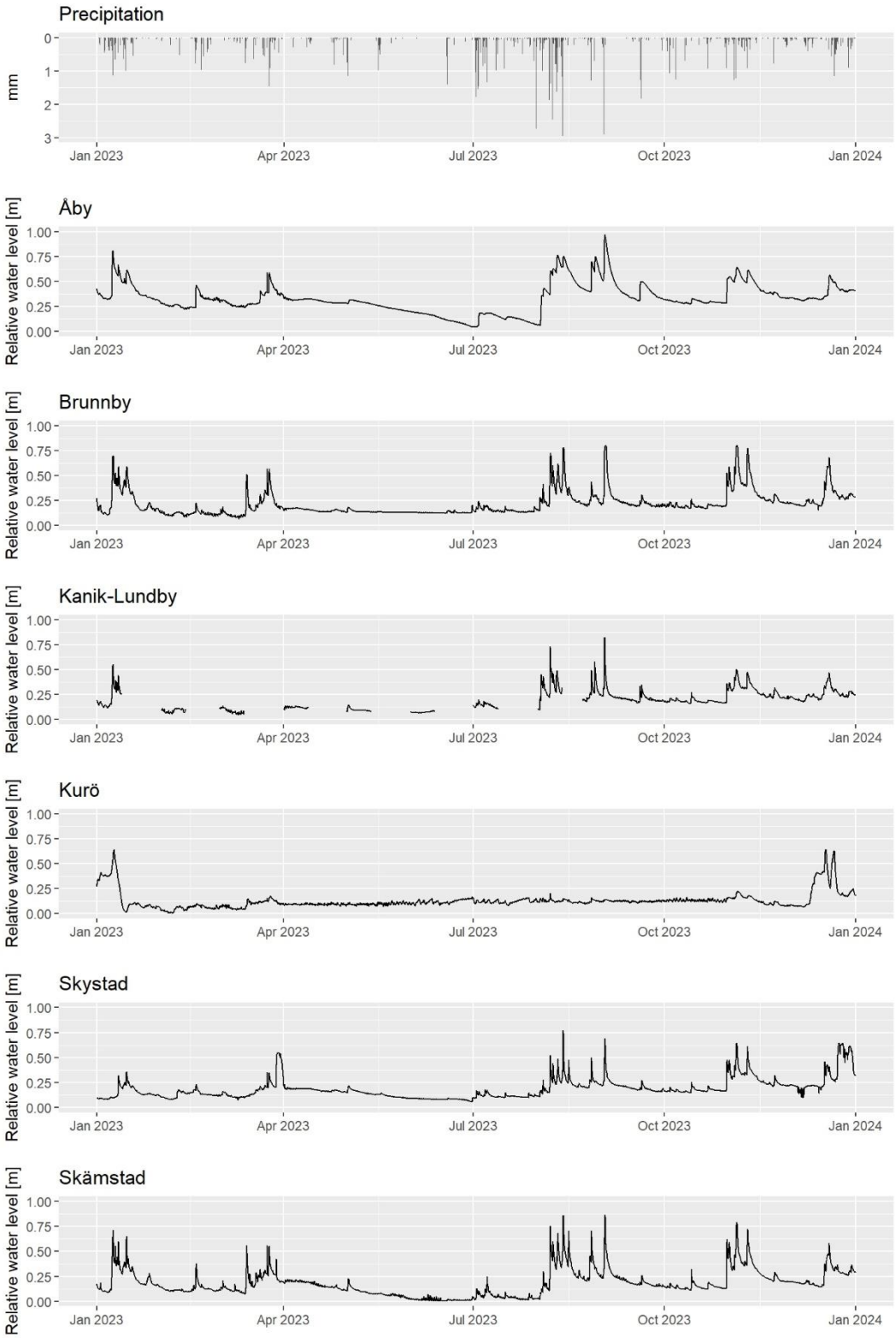

Figure 4. Relative water level data plotted against precipitation data for CW in Västmanland County for the year 2023. Missing values indicate removed outliers.

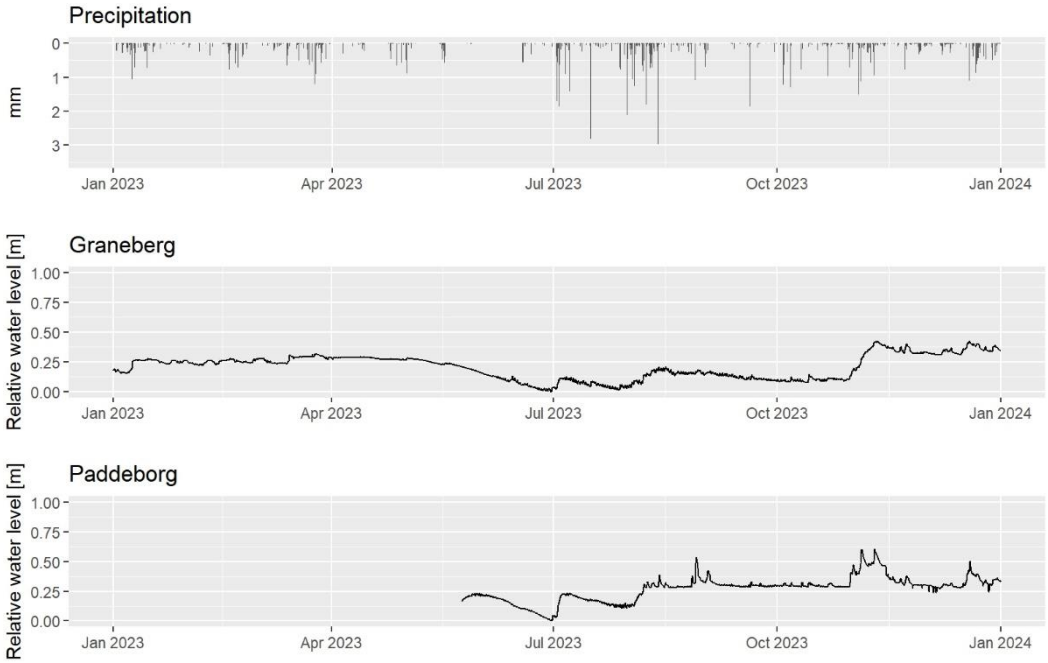

Figure 5. Relative water level data plotted against precipitation data for CW in Uppsala County for the year 2023. Missing values indicate removed outliers.

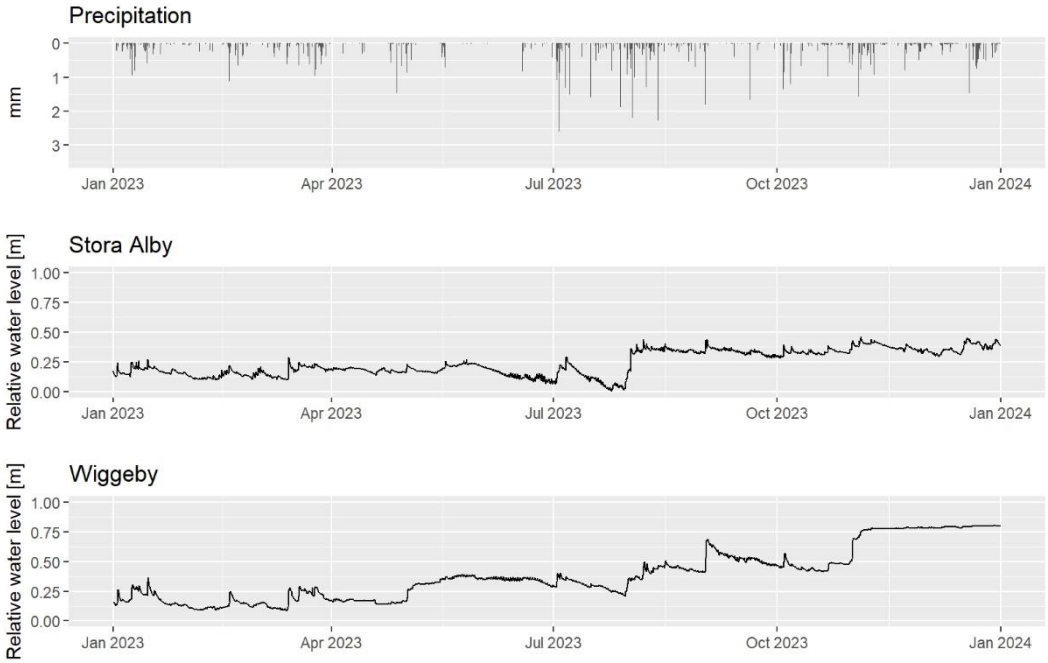

Figure 6. Relative water level data plotted against precipitation data for CW in Stockholm County for the year 2023. Missing values indicate removed outliers.

3.2 Monte Carlo analysis

MC results for Aby, Bru and Gra (see Appendix, figures 13-21) show that all ponds have similar sensitive parameters, mainly threshold temperatures for rain/snow, relative
amounts of water moving between boxes, boxes characteristic time constants, parameters controlling evaporation rates, parameters for estimating stream depth and retained water depth.
After three runs of MC analysis the ensembles of best performing parameter sets all showed a Nash-Sutcliffe efficiency higher than 0.61 (table 4).

Table 4. Nash-Sutcliffe efficiency for the best and the worst performing parameter set in the ensemble of the ten best performing parameter sets for Aby, Bru and Gra.

Ensemble of best performing parameter sets	**Åby**	**Brunnby**	**Graneberg**
Highest NSE	0.686	0.622	0.698
Lowest NSE	0.677	0.614	0.687

3.3 Future climate scenarios

Mean water levels [m] for the period 2041-2070 were calculated from the modelling results of the ten best performing parameters sets for the baseline and the 11 different future climate scenarios are visualized for Aby, Bru and Gra in figures 8-10. Due to the amount of data (hourly values for 30 years) a visualization of a minimum and maximum range for the different scenarios was not feasible (see Appendix, figure 22).

For Aby (figure 8), the baseline scenario shows that the mean relative water level ranges between 0.2-0.6 m, and patterns show tendencies of drying out phases in summer and recharging phases in fall. Some years are more extreme than others without an obvious pattern. The water level pattern of RCP4.5 is in a similar range only slightly higher. For RCP4.5 the largest deviations can be found for RCP4.5_Stretch3 with a range of 0.25-1.00 m. RCP8.5's relative water level is also closest to the baseline scenario, whereas the amplitude of water level changes of RCP8.5_Stretch4 is the highest (0.25-1.00 m). The Stretch1 to Stretch3 demonstrate the highest average differences compared to the baseline scenario with smallest ranging from 0.25-0.75 m (Stretch1) and from 0.25-1.00 m (Stretch2).

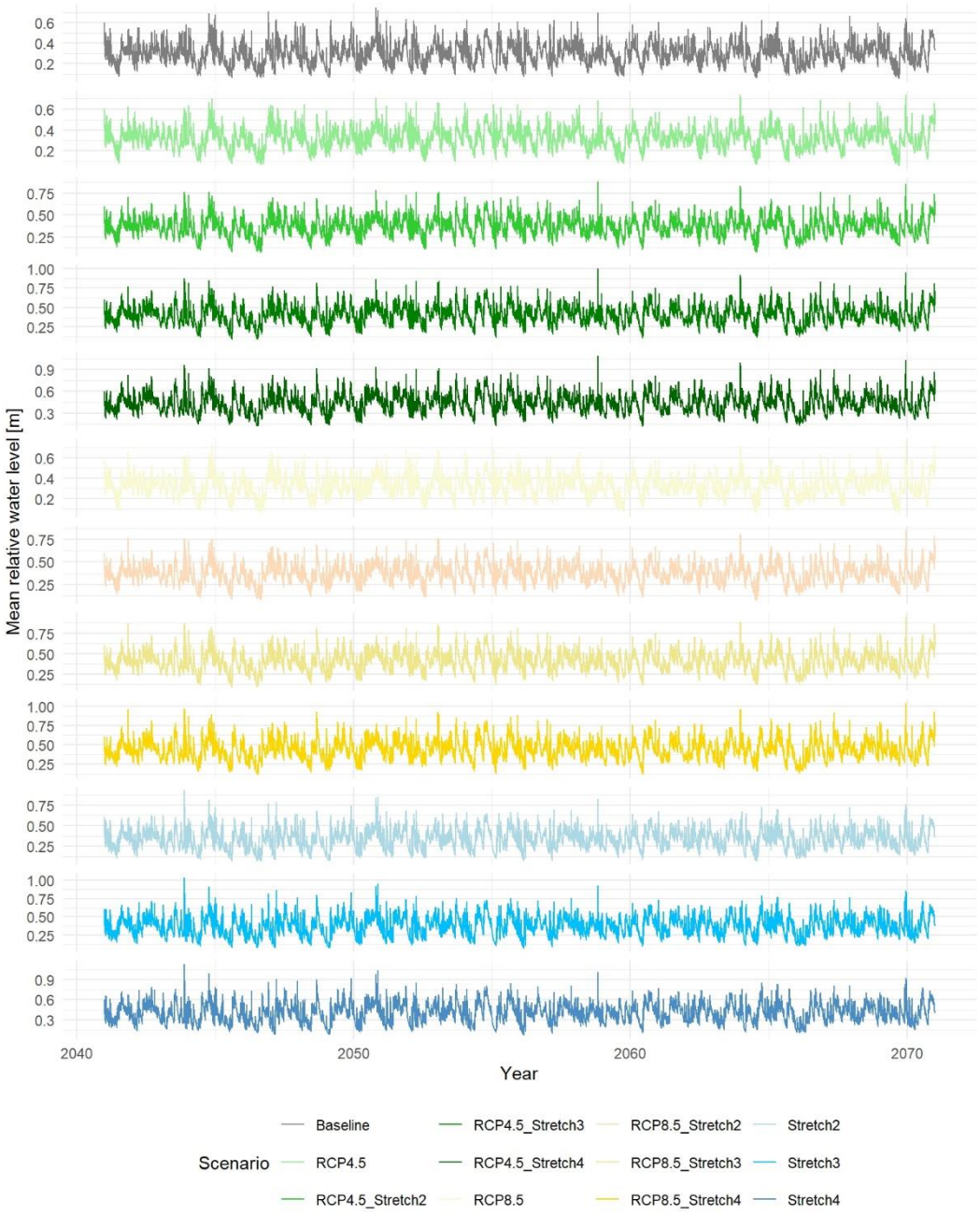

Figure 7. Projected mean water level [m] for Aby for the baseline scenario and the different future climate scenarios for the period 2041-2070.

Equally, minimum, mean and maximum relative water level for Aby grouped for the four different seasons (figures 9a-c) show all a similar tendency. The median value and the box itself shift for every scenario higher with a higher stretch scenario compared to the baseline scenario. Relative water levels in winter and spring appear to be more stable than relative water levels in summer and fall, where they fluctuate in a wider range. Summer presents the least outliers, whereas all scenarios show a wide range of outliers in the upper section.

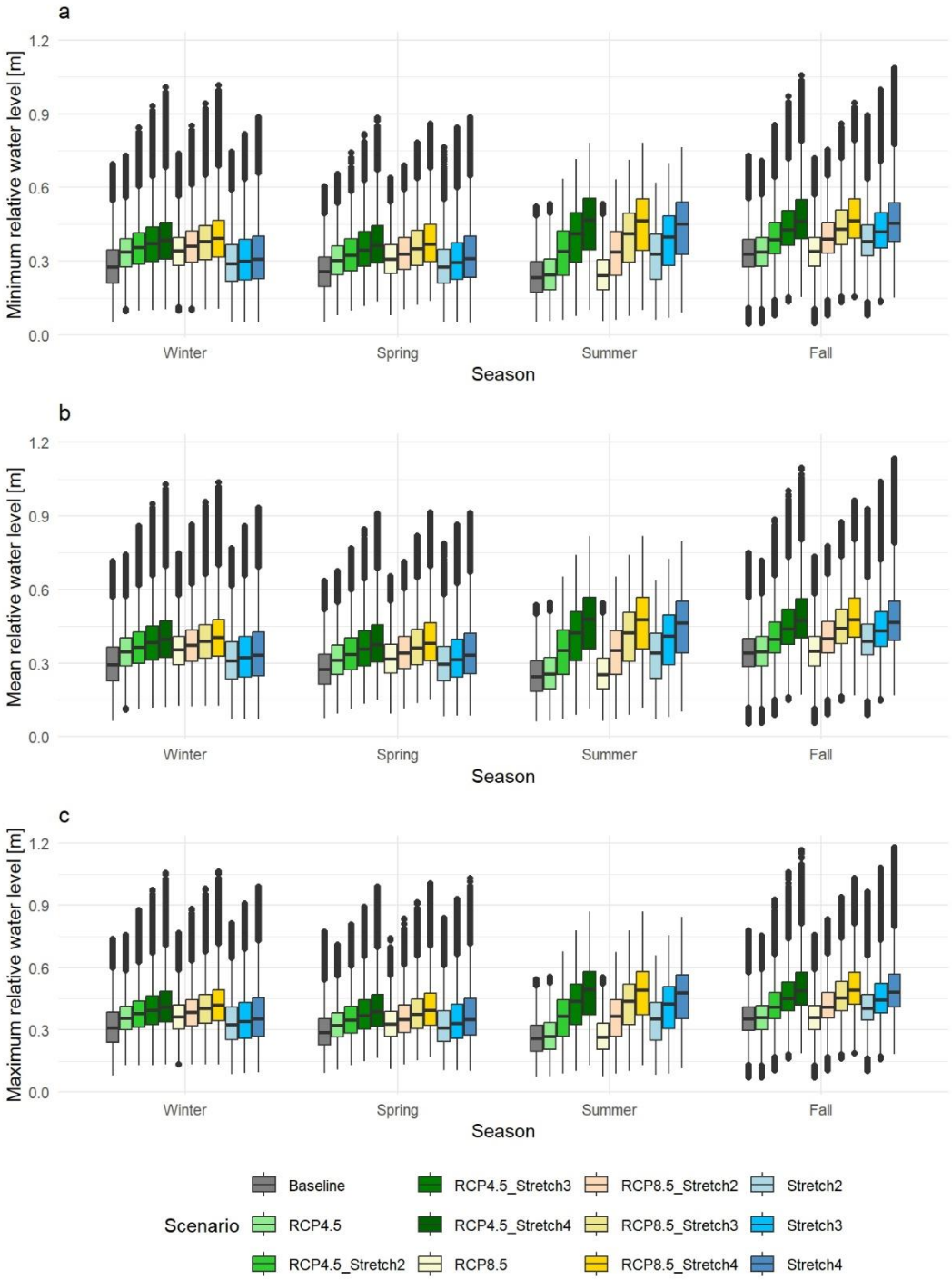

Figure 8. a) Minimum relative water level of ensemble data grouped by season (winter, spring, summer, fall) for Aby for the period 2041-2070. b) Mean relative water level of ensemble data grouped by season (winter, spring, summer, fall) for Aby for the period 2041-2070. c)Maximum relative water level of ensemble data grouped by season (winter, spring, summer, fall) for Aby for the period 2041-2070.

Mean relative water level for the baseline scenario of Bru (figure 10) varies from approximately 0.2-0.6 m. Drying out phases are not as distinct compared to the ones in Aby but therefore peak water levels are higher. Water level for the RCP4.5

scenario differs between 0.2-0.6 m but with a lower overall amplitude, while RCP4.5_Stretch2 and RCP4.5_Stretch4 present the highest variation of mean water level of 0.2-0.8 m and 0.25-0.75 m respectively.

RCP8.5 and its stretches have a smaller variation compared to the different RCP4.5 scenarios with the highest ranging from 0.2-0.8 m (RCP8.5_Stretch3).

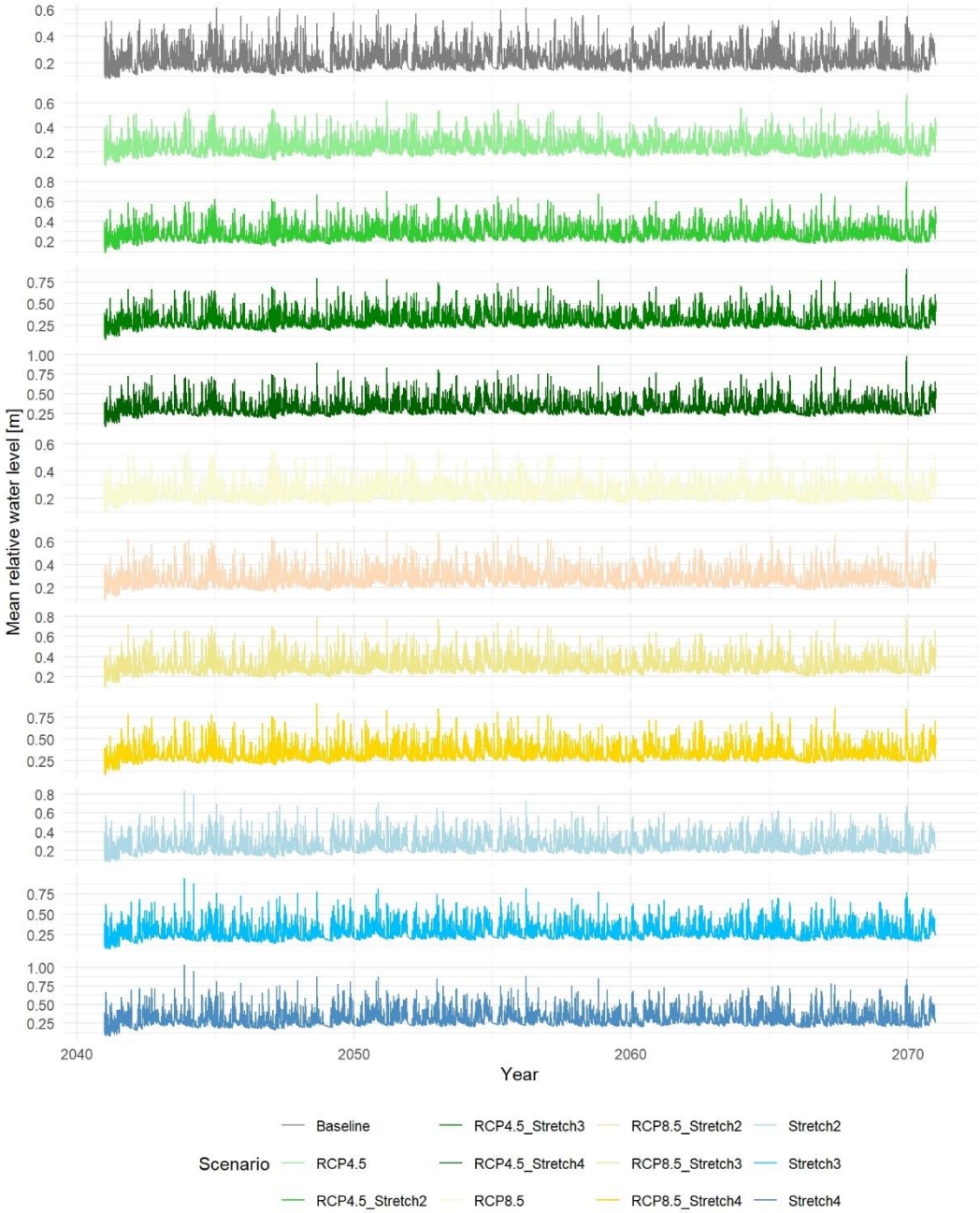

Figure 9. Projected mean water level [m] for Bru for the baseline scenario and the different future climate scenarios for the period 2041-2070.

Amplitude of mean water level for Stretch3 scenario is smallest with a range of 0.25-0.75 m, whereas amplitudes of Stretch2 (0.2-0.8 m) and Stretch4 (0.25-1.00 m) are higher.

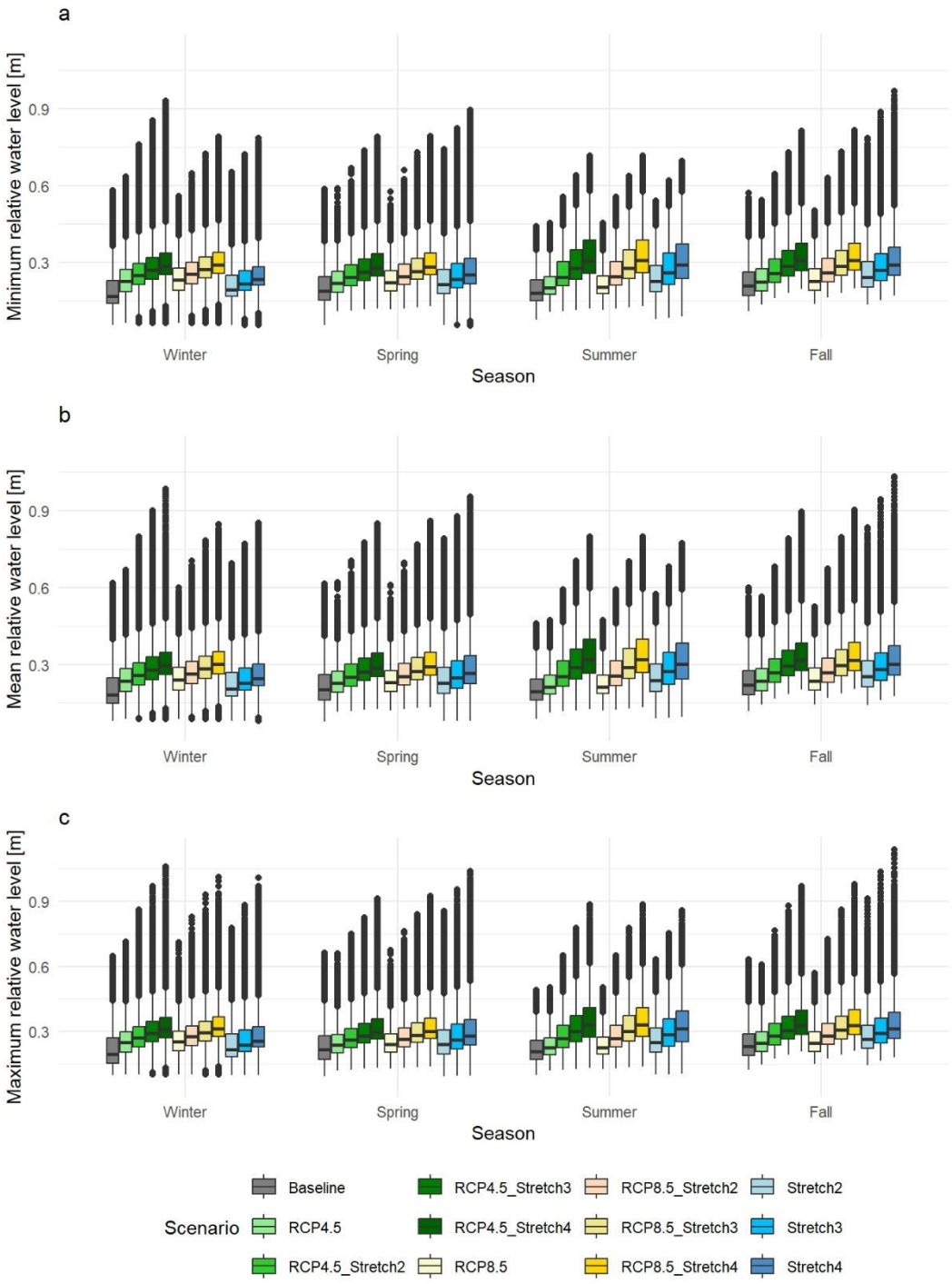

Figure 10. a) Minimum relative water level of ensemble data grouped by season (winter, spring, summer, fall) for Bru for the period 2041-2070. b) Mean relative water level of ensemble data grouped by season (winter, spring, summer, fall) for Bru for the period 2041-2070. c)Maximum relative water level of ensemble data grouped by season (winter, spring, summer, fall) for Bru for the period 2041-2070.

This is also reflected in results shown in figure 11a-c. Boxplots for all seasons behave similarly across the minimum, mean and maximum values.

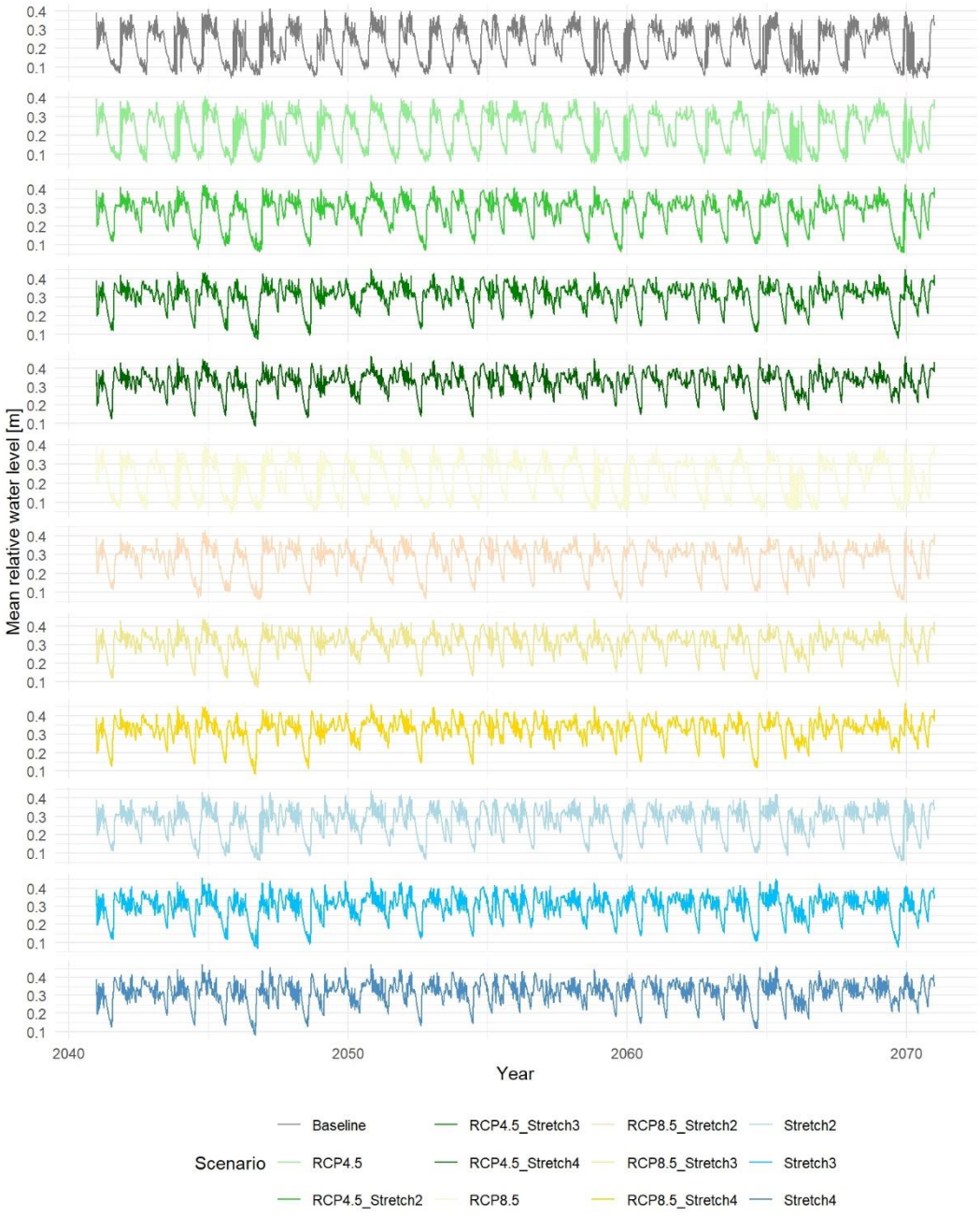

Figure 11. Projected mean water level [m] for Gra for the baseline scenario and the different future climate scenarios for the period 2041-2070.

Graneberg's (figure 10) baseline scenario exhibits the most pronounced and largest drying out periods over summer for multiple months with a complete recharge starting approximately in September every year with a mean water level between 0.1-0.4 m.

RCP4.5 and all the RCP4.5_Stretch scenarios differ in the same range as the baseline period. RCP4.5 shows a very similar behaviour regarding the decrease and

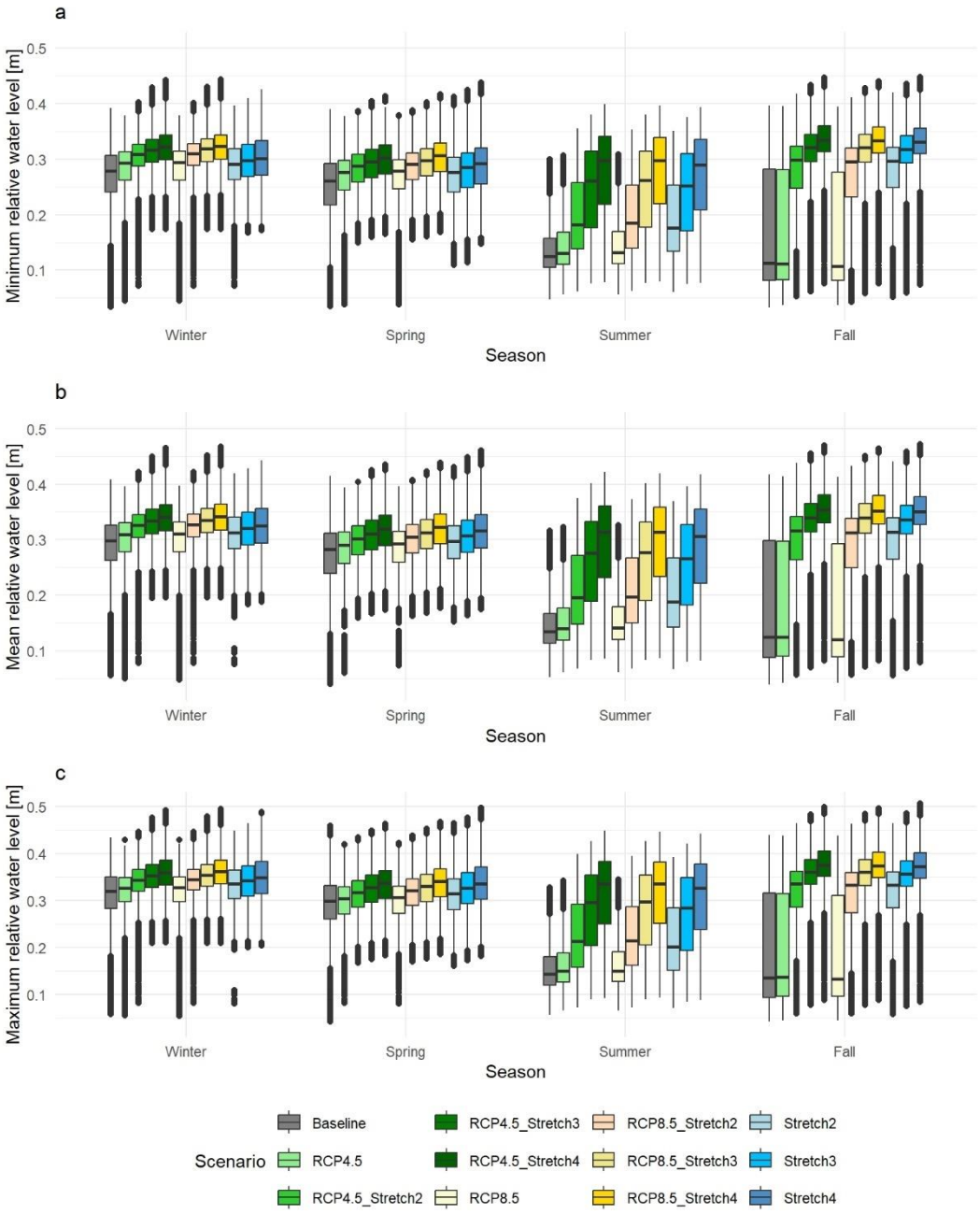

Figure 12. a) Minimum relative water level of ensemble data grouped by season (winter, spring, summer, fall) for Gra for the period 2041-2070. b) Mean relative water level of ensemble data grouped by season (winter, spring, summer, fall) for Gra for the period 2041-2070. c)Maximum relative water level of ensemble data grouped by season (winter, spring, summer, fall) for Gra for the period 2041-2070.

increase in the summer month, but with increasing stretches the drying out phases appear to be shorter and not as strong. RCP8.5 and the different stretch scenarios

act similarly as RCP4.5 scenarios, the higher the stretch the shorter the drying out period and the smaller the amplitude with all scenarios varying from 0.1-0.4 m.

This pattern also be observed in figure 13a-c. There it becomes obvious that the most distinctive changes happen in summer and fall. RCP4.5 and RCP8.5 only behave equally to the baseline scenario with a wide spread of the box. With higher stretches the boxes become more compact and with more outliers in the lower range.

One observation that can be made for all ponds is that none will dry out completely in the baseline nor in any of the future climate scenarios.
Moreover, the results of this study show that RCP4.5 and RCP8.5 alone will not cause major shifts of minimum, mean or maximum relative water levels across seasons compared to the baseline scenario for the subset of the tree ponds Aby, Bru and Gra. Major shifts were detected for all ponds with higher extreme precipitation stretch scenarios as well when there were performed under projected RCP4.5 and RCP8.5 scenarios. Missing outliers indicate that relative water level in Aby is relatively stable in summer compared to the other seasons. Bru shows a varying amplitude with a tendency for outliers within the upper range throughout the year whereas Gra's relative water level patterns present the opposite. The outliers concentrated in the lower range apart from summer. Additionally, boxes, whiskers and outliers indicate a strong variation in relative water level, which is confirmed by the different water level curves.

4. Discussion

4.1 PERSiST feasibility

Firstly, feasibility of PERSiST needs to be assessed. Semi-distributed conceptual models lack spatial heterogeneity of catchments which is amplified due to forming sub catchment areas. This generalization results in a resolution deficit, eventually causing space for uncertainty. Regardless their deficiencies semi-distributed process-based model offer profound assets such as a simple model structure, an easy calibration possible with only limited data availability and fewer computational power needed to operate (Jehanzaib *et al.*, 2022). No model type is free from uncertainty, therefore choosing the right one depends on the modeller's specific research question(s) and prerequisites (Sitterson *et al.*, 2018).
This study focuses on a multi-setup-approach resembling different kinds of CW based on one conceptual model (figure 7), which is achieved through the box structure that allows to turn certain boxes on and off as needed. Though the overall catchment setup is simple only considering one land cover class and basic pond characteristics, a good model fit between modelled and observed data was achieved (NSE > 0.61) for all three ponds (table 4). Given these overall satisfying model performances using only one conceptual model is a good approach to model water level dynamics for different ponds until the main drivers for their behaviour is better understood.

It is to mention though that for Gra NSE alone was not reliable to determine good model fit as the modelled pattern deviated too much from the observed one. Thus, an inspection was necessary to guarantee both a good statistical and visual fit (see Appendix, figure 23).

Subsurface and surface processes and connectivity of wetlands are still poorly understood even for wetlands with similar geographical characteristics (McLaughlin *et al.*, 2019). PERSiST allows altering the properties of the buckets and arrangement of the hydrological response units flexibly so the diverse patterns of the CW can be depicted. Nonetheless the over-deterministic character of PERSiST must be emphasized, meaning that the same output time series can be

achieved with different combinations of input parameters. On the other hand the number of possible input parameters allows to imply more processes that are potentially necessary to reproduce the observed behaviour compared to other models (Futter *et al.*, 2015).

The small size of the catchments (< 2.5 km^2) prevents the loss of principal landscape characteristics even though averaging the data. Moreover, PERSiST can be understood quickly due to its user-friendliness and low-threshold input requirements (Futter *et al.*, 2015).

Additionally, hourly data for a 30-year period for several different future change scenarios needs to be run which also was successfully executed by PERSiST without the need for high-computational resources but a regular computer (Microsoft Surface Pro 5^{th} generation from 2017).

Although it is originally not especially designed to depict water level changes for constructed wetlands but rainfall runoff patterns in river and stream catchments PERSiST allows to calibrate against water depth and hence making it a suitable model approach. In addition to this, different model approaches to estimate water storage capacities for ponds were found, either holistic, using the Soil Water Assessment Tool or remote sensing but none fulfilled the requirements of an easy application and as few input requirements as good as PERSiST (Ali *et al.*, 2015; S. Chen *et al.*, 2020; W. Chen *et al.*, 2020).

All the mentioned above shows that within the research question and aims PERSiST is a suitable program to model future climate scenarios for water level patterns and thus water storage capacity.

4.2 Developing future climate scenarios

Precipitation is one of the main components of the hydrological cycle and hence a driving force in the behaviour of CW's hydrology. Therefore, it is of utmost importance to have consistent long-term precipitation datasets with high temporal and spatial resolution assessing hydrological behaviour, especially extreme precipitation events (Longo-Minnolo *et al.*, 2022).

Climate data is historically derived from instrumental in situ observations. Measurements made by gauging stations do not often meet these requirements due to susceptibility to different errors, insufficient spatial distribution to reproduce the climate variability of precipitation events and time lagging (Ledesma and Futter, 2017; Grusson and Barron, 2022). Olsson *et al.* (2019) showed that high temporal

resolution data just started to be taken by an automatic network in Sweden between 1995-1996 and though overall coverage is satisfying data gaps remain.

To avoid these deficiencies, gridded ERA5-Land data was used for calibration of the models and developing the different future climate scenarios. Médus *et al.* (2022) reported an underestimation of spread of average precipitation, precipitation intensities in general but particularly for extreme precipitation events for hourly ERA5 datasets in the Nordic region implying Sweden due to a too coarse grid (31 km).

ERA5-Land data is the successor to ERA5 and was further downscaled to a spatial resolution of 9 km to tackle the issue of too coarsely gridded data (Muñoz-Sabater *et al.*, 2021). This advancement allows to reproduce climate behaviour satisfyingly on a watershed scale but for a broader temporal scope as it still underestimates extreme events (Grusson and Barron, 2022; Longo-Minnolo *et al.*, 2022). Longo-Minnolo *et al.* (2022) carried out a correction using local measurements and could reduce the precipitation underestimation discrepancy significantly from 25 % to 7 %.

A correction with in situ observations in Mälardalen of ERA5-Land data was not performed in this study, but to take the known issue of precipitation underestimation into account, the extreme precipitation stretch scenarios were multiplied by 200, 300 and 400 % compared to the baseline scenario. These numbers may appear to be exaggerated at first glance, but ERA5-Land was not able to even closely reproduce extreme events, e.g. the flooding in Uppsala July 29th 2018 with more than 80 mm of precipitation in a day (Forsell, 2018). Hence, to realistically project future climate scenarios the stretches were performed in the above-described magnitude.

The results of RCP4.5 and RCP8.5 scenario calculation derived from SMHI regional ensemble data show an increase in temperature and precipitation across all seasons, which is higher for RCP8.5 than for RCP4.5. Driving data that was generated for this study is consistent with IPCC projections (IPCC, 2021, 2022) and therefore appears to be a legitimate way of modelling future climate scenarios in small catchment areas without consuming too much time and computational resources. Additionally, it needs to be mentioned that it remains a major challenge to approximate intensity and frequency of extreme precipitation events even with large ensemble projections (Chen *et al.*, 2015).

Keeping these constraints in mind, the overall approach of creating the future climate scenarios seems like a good way with minor trade-offs to have readily data available.

4.3 Flood buffering capacity under future climate scenarios

Relative water level can be used as proxy to determine the flood buffering capacity of a wetland, a property describing the ability of a wetland to reduce and prevent floodings. The time in which water level increases can be defined as single buffering event. All buffering events over a certain period, e.g. a year, equalled up describe the total buffering capacity of a wetland (Åhlén *et al.*, 2022; Strand *et al.*, 2024).
Although water storage capacity was not actively included in this study by calculating the volume of the ponds or considering the bathymetry, it is still not completely neglected. This study calibrated against water level, which is dependent on physical limitations of a wetland and therefore also its shape and its volume. Additionally, PERSiST is a model reproducing streamflow patterns. Routing the water through different boxes reproduces the water level at the same time. The model will do so based on first-difference equations and parameter inputs like reach length and width at sediment surface and will deliver more accurate results than bathymetry measurements that were made once and only depict this certain moment. Therefore, using relative water level to describe flood buffering capacity in this study is a reasonable approach.

Results in this study have shown that relative water level is shifting upwards with RCPs combined with extreme precipitation stretch scenarios in winter and spring months, but variation is little compared to spring and fall months. Like previous studies (Thorslund *et al.*, 2017; Åhlén *et al.*, 2022) focus will on the summer half of the hydrological year.

Gra's relative water level pattern presents by far the most particular behaviour regarding drying out and regeneration phases in summer and fall whereas relative water level curves for the different scenarios in Bru show the least amplitude and variation. Relative water level curves in Aby present a pattern in between the other two ponds.

This could be connected to their location in the landscape, meaning that Gra is situated downstream, thus receiving less water and showing these extensive drying out periods and having a greater buffering capacity in extreme flooding events

(Quin and Destouni, 2018; Åhlén *et al.*, 2022). Regarding the observed relative water level pattern in 2023 and precipitation data (figure 7), this seems to be even more accurate as water levels only increase slowly over the summer months but over proportionally rapid in fall.

Moreover, Graneberg as a biodiversity pond and therefore not designed to be linear but more twisted, also including islands in the middle of the CW to guarantee a slow and steady raise in water level to enhance the living conditions for different species there. This is done by creating a large relative area compared to the whole catchment area. Gra as CW has with 5.24 % (table 1) by far the largest relative area compared to Bru (0.12 %) and Aby (0.07 %).

Due to that small relative area of Aby's and Bru's CWs their response of mean water level to stronger precipitation events is therefore less delayed and more pronounced (figure 6).

The fact that Bru does not seem to be sensitive to drying out periods under present or future climate conditions can be related to different reasons. It is a P-retention pond in an agricultural dominated landscape (84 %). Hence, the surrounding fields constantly drain into the CW keeping its relative water level constant even throughout drier periods.

Furthermore, Bru is in close proximity to a groundwater magazine (< 1 km). A shallow groundwater table or other surface and subsurface water bodies could be responsible for the stable water level in dry phases, too (McLaughlin, Kaplan and Cohen, 2014; Ameli and Creed, 2017; Thorslund *et al.*, 2017, 2018). Bru is designed in a more linear shape with steeper edges causing a faster increase of water level in precipitation events. All the mentioned above impacts Bru's flood buffering capacity negatively, not allowing too much water to be stored. However, this design could be beneficial in dry spells (e.g. keeping a water surface for animals in an otherwise dry landscape).

The CW in Aby is a P-retention pond though unique due to its setup within a stream. Similarly to Bru, relative are of Aby is very small and the dominating land cover class is agriculture (54 %). Though Aby behaves in drier periods differently as the water level decreases. This suggests that there is not sufficient drainage from the surrounding environment into the CW to keep the water level constant and/ nor interactions with other subsurface water bodies which is underlined by the distance to the closest groundwater magazine (5-10 km). It offers a higher flood buffering capacity than Bru in dry periods but not as high as Gra.

The results of the future climate scenarios for RCP4.5 and RCP8.5 scenarios alone appear not to impact the relative water level much, indicating that the ponds would be resilient against temperature and precipitation increase and could be used as a nature-based solution against floods. Whereas the stretch scenarios cause a major increase in minimum, mean and maximum relative water level. Consequently, water storage capacity decreases and hence their flood buffering capacity, too.

4.4 Limitations

Due to an overall time limitation the following aspects were not or not sufficiently assessed and should be included in future research.

4.4.1 Calibration period

Hourly air temperature and precipitation ERA5-Land data for 2023 was used to calibrate the observed data against to. This decision was made for practical reasons as it was not yet proven that PERSiST can operate 30 years of hourly data. Additionally, download and processing this amount of data would have taken too much time. Thus, the calibration process was performed only with data from 2023 as measurements were also taken in 2023.
It needs to be emphasized that 2023 was a year coined by extreme meteorological events such as a long and hot phase in summer followed by an extended period with a lot of precipitation.
To balance those events and reproduce a more consistent picture a longer period should be employed to perform the calibration in the future. As feasibility was demonstrated by this study, future calibration should use a period of 30 years at an hourly timestep.

4.4.2 Statistical evaluation

Equally to extreme climate events, it is of more interest how CWs will perform under extreme conditions and what their response is to those extremes. Therefore, the tail of probability distribution needs to be assessed further as extremes are depicted there. To do so extreme value theory seems like an appropriate approach as it is a widely used method in environmental and hydrological modelling to generally base managing decisions on (fig. 14). Further, the Generalized Extreme Value distribution, the Peak-Over-Threshold methods or the Metastatistical Extreme Value distribution are different approaches with different advantages and disadvantages (Renard and Lang, 2007; Feng *et al.*, 2018; Gründemann *et al.*, 2023). Evaluating these lays beyond the scope of this work though.

4.4.3 Relative water level as proxy for water storage capacity

This study assumes that water level functions as indicator for water storage capacity of a CW as well as its flood buffering capacity. To strengthen this assumption and gain a more reliable output actual water storage capacity should be calculated. As no measurements of streamflow have been taken in the past or present estimating actual water storage capacity of an CW like Åhlén *et al.* (2022) is not feasible.
Instead, latest techniques like remote sensing could be used as high-resolution, airborne light detection and ranging (LiDAR) data is more easily accessible. Based on these information not only actual but also potential water storage capacity could be estimated (Jones *et al.*, 2019; Papa and Frappart, 2021).

4.4.4 Policy and design recommendations

Regarding a changing climate CWs can function as a nature-based solution to improve resilience against floods in a landscape (Thorslund *et al.*, 2017). It is important to implement smart and effective designed CWs in the present but to do so more data is needed to understand mechanisms and processes behind interactions of CWs and its environment even more to project findings on a larger scale (Park *et al.*, 2014; Jones *et al.*, 2019). To better characterize the ten CWs in Mälardalen better and create a more consistent picture, future research and model setup should imply more data about topographical, land use and management. Especially management decisions should be regarded as these CWs are all anthropogenically influenced in different ways. Accordingly, this study is not able to give any suggestions on how policies or pond designs should be made.

Nonetheless, it appears that current policies and pond designs are resilient to an overall increase in temperature and precipitation as RCP4.5 and RCP8.5 project. Further data should therefore be used to assess climate-smart designs under extreme precipitation events. How to handle those and guarantee that the ponds successfully buffer floods will be a major obstacle and should therefore be focused on by the research community in the near future.

5. Conclusions

Climate change will cause alterations in precipitation intensities and frequencies as well in temperature. CWs could be a potential mitigation measure and create more resilience in the environment to encounter those future changes.
Thus, it was the overall objective of this study to model water storage capacity of small CWs in Mälardalen under present and future climate scenarios using relative water level changes as proxy. The results led to the following conclusions:

(a) The design of the conceptual model includes several components – direct runoff, upper soil water, lower soil water, upper groundwater, riparian unsaturated zone, lower groundwater and wetland. This structure was successfully translated into a square matrix defining the water flows between boxes in PERSiST. This multi-setup approach allowed to satisfyingly reproduce the water level changes of observed measurements of the different ponds.

(b) Using hourly ERA5-Land and SMHI regional ensemble data for the respective counties the CWs are in for the seasons winter, spring, summer and fall a baseline scenario, RCP 4.5 and RCP8.5 as well as extreme precipitation stretch scenarios were produced. The method used permitted to obtain scenarios with a high temporal resolution (hourly data for a period of 30 years) not depending on high-computational power or a long generation time. The results for the RCP4.5 and RCP8.5 show an increasing trend in temperature and precipitation, which is consistent with other projections for those scenarios in Sweden. Extreme stretches accounted for the underestimation of precipitation events of ERA5-Land data by choosing a higher multiplier and were able to project extreme precipitation scenarios. Making it a feasible method to project future climate scenarios.

(c) PERSiST originally designed to model streamflow or runoff of streams and rivers at a daily timestep, was used the first time to model water level changes of wetlands using driving data with an hourly timestep for a 30-year period for a subset of three ponds. Model outputs suggest that none of ponds in the subset will dry out under any future climate scenarios.

Additionally, all water level patterns of all CWs reacted the least to the RCP4.5 and RCP8.5 scenarios alone compared to the baseline scenario. Only together with the extreme precipitation stretches the behaviour of relative water level presented an upward shift. Strongest differences were observed in summer and fall with pronounced drying out and regeneration phases for Gra compared to the Aby and Bru. Reasons for these different patterns can most likely be due to pond purpose and its respective design, relative area compared to catchment size and surrounding land cover class. Interactions with other subsurface water bodies like close groundwater magazines cannot neither be excluded nor confirmed. All this leads to the conclusion that Graneberg has the highest flood buffering capacity followed by Aby and lastly by Bru.

Several limitations were encountered in this study that should be considered in future research.

- Extreme distribution of relative water level was not statistically assessed. Behaviour of extreme events is of special interest, thus an extreme value distribution approach should be used to investigate those patterns.

- Relative water level changes were used as proxy for water storage and hence flood buffering capacity in this study without including further parameter confirming this. As streamflow measurements are not feasible, LiDAR data should be used to estimate actual and potential water storage capacity, connect it to relative water level changes, and reproduce flood buffering capacity in a more consistently.

- Further data and measurements are needed to reliably recommend smart and efficient wetland design, management and policy solutions.

References

Åhlén, I. *et al.* (2021) 'Hydro-climatic changes of wetlandscapes across the world', *Scientific Reports*, 11(1), p. 2754. Available at: https://doi.org/10.1038/s41598-021-81137-3.

Åhlén, I. *et al.* (2022) 'Wetland position in the landscape: Impact on water storage and flood buffering', *Ecohydrology*, 15(7), p. e2458. Available at: https://doi.org/10.1002/eco.2458.

Ali, S. *et al.* (2015) 'A holistic water depth simulation model for small ponds', *Journal of Hydrology*, 529, pp. 1464–1477. Available at: https://doi.org/10.1016/j.jhydrol.2015.08.035.

Althoff, D. and Rodrigues, L.N. (2021) 'Goodness-of-fit criteria for hydrological models: Model calibration and performance assessment', *Journal of Hydrology*, 600, p. 126674. Available at: https://doi.org/10.1016/j.jhydrol.2021.126674.

Ameli, A.A. and Creed, I.F. (2017) 'Quantifying hydrologic connectivity of wetlands to surface water systems', *Hydrology and Earth System Sciences*, 21(3), pp. 1791–1808. Available at: https://doi.org/10.5194/hess-21-1791-2017.

Chen, D. *et al.* (2015) 'Projecting future local precipitation and its extremes for sweden', *Geografiska Annaler: Series A, Physical Geography*, 97(1), pp. 25–39. Available at: https://doi.org/10.1111/geoa.12084.

Chen, S. *et al.* (2020) 'A new method to improve the accuracy of remotely sensed data for wetland water balance estimates', *Journal of Hydrology: Regional Studies*, 29, p. 100689. Available at: https://doi.org/10.1016/j.ejrh.2020.100689.

Chen, W. *et al.* (2020) 'Exploring the multiscale hydrologic regulation of multipond systems in a humid agricultural catchment', *Water Research*, 184, p. 115987. Available at: https://doi.org/10.1016/j.watres.2020.115987.

Coppola, E. *et al.* (2021) 'Assessment of the European Climate Projections as Simulated by the Large EURO-CORDEX Regional and Global Climate Model Ensemble', *Journal of Geophysical Research: Atmospheres*, 126(4), p. e2019JD032356. Available at: https://doi.org/10.1029/2019JD032356.

Costanza, R. *et al.* (2014) 'Changes in the global value of ecosystem services', *Global Environmental Change*, 26, pp. 152–158. Available at: https://doi.org/10.1016/j.gloenvcha.2014.04.002.

Crespi, A. *et al.* (2020) 'Climate-related hazard indices for Europe'. Available at: https://doi.org/10.25424/CMCC/CLIMATE_RELATED_HAZARD_INDICES_EUROPE_2020.

Cui, Q. *et al.* (2021) 'Regional wetland water storage changes: The influence of future climate on geographically isolated wetlands', *Ecological Indicators*, 120, p. 106941. Available at: https://doi.org/10.1016/j.ecolind.2020.106941.

Deutscher, J., Hemr, O. and Kupec, P. (2021) 'A Unique Approach on How to Work Around the Common Uncertainties of Local Field Data in the PERSiST Hydrological Model', *Water*, 13(9), p. 1143. Available at: https://doi.org/10.3390/w13091143.

European Commission (2000) 'Directive (EU) 2018/ of the European Parliament and of the Council of 30 May 2018 amending Directive 2008/98/EC on waste'.

European Commission (2007) *LIFE and Europe's wetlands : restoring a vital ecosystem*. LU: Publications Office. Available at: https://data.europa.eu/doi/10.2779/22840 (Accessed: 3 May 2024).

Evenson, G.R. *et al.* (2016) 'An improved representation of geographically isolated wetlands in a watershed-scale hydrologic model', *Hydrological Processes*, 30(22), pp. 4168–4184. Available at: https://doi.org/10.1002/hyp.10930.

Feng, J. *et al.* (2018) 'How to apply the dependence structure analysis to extreme temperature and precipitation for disaster risk assessment', *Theoretical and Applied Climatology*, 133(1–2), pp. 297–305. Available at: https://doi.org/10.1007/s00704-017-2187-5.

Forsell, D. (2018) 'Regnrekord i Uppsala – "Ovanligt med så mycket regn på så kort tid"', 30 July. Available at: https://www.svt.se/nyheter/lokalt/uppsala/kraftiga-regnet-i-uppsala-ovanligt-med-sa-mycket-regn-pa-sa-kort-tid.

Futter, M.N. *et al.* (2014) 'PERSiST: a flexible rainfall-runoff modelling toolkit for use with the INCA family of models', *Hydrology and Earth System Sciences*, 18(2), pp. 855–873. Available at: https://doi.org/10.5194/hess-18-855-2014.

Futter, M.N. *et al.* (2015) 'Rainfall runoff modelling of the Upper Ganga and Brahmaputra basins using PERSiST', *Environmental Science: Processes & Impacts*, 17(6), pp. 1070–1081. Available at: https://doi.org/10.1039/C4EM00613E.

Golden, H.E. *et al.* (2014) 'Hydrologic connectivity between geographically isolated wetlands and surface water systems: A review of select modeling methods', *Environmental Modelling & Software*, 53, pp. 190–206. Available at: https://doi.org/10.1016/j.envsoft.2013.12.004.

Graversgaard, M. *et al.* (2021) 'Policies for wetlands implementation in Denmark and Sweden – historical lessons and emerging issues', *Land Use Policy*, 101, p. 105206. Available at: https://doi.org/10.1016/j.landusepol.2020.105206.

Gründemann, G.J. *et al.* (2023) 'Extreme precipitation return levels for multiple durations on a global scale', *Journal of Hydrology*, 621, p. 129558. Available at: https://doi.org/10.1016/j.jhydrol.2023.129558.

Grusson, Y. and Barron, J. (2022) 'Challenges in reanalysis products to assess extreme weather impacts on agriculture: Study case in southern Sweden', *PLOS Climate*. Edited by S.V. Raghavan, 1(9), p. e0000063. Available at: https://doi.org/10.1371/journal.pclm.0000063.

Hambäck, P.A. *et al.* (2023) 'Tradeoffs and synergies in wetland multifunctionality: A scaling issue', *Science of The Total Environment*, 862, p. 160746. Available at: https://doi.org/10.1016/j.scitotenv.2022.160746.

Hill, M.J. *et al.* (2021) 'Pond ecology and conservation: research priorities and knowledge gaps', *Ecosphere*, 12(12), p. e03853. Available at: https://doi.org/10.1002/ecs2.3853.

Intech Instruments (no date) 'Water level / Temperature Data Logger. Logger Model WT-HR mark 3 Three Channel High Resolution (12 bit) Water level / Temperature Data Logger.' Available at: https://www.intech.co.nz/wp-content/uploads/TruTrack-WT-HR-Series-Water-Level-Temperature-Logger-Data-Sheet_IN160721.pdf (Accessed: 3 June 2024).

IPCC (2021) *Climate Change 2021 – The Physical Science Basis: Working Group I Contribution to the Sixth Assessment Report of the Intergovernmental Panel on Climate Change*. 1st edn. Cambridge University Press. Available at: https://doi.org/10.1017/9781009157896.

IPCC (2022) *Climate Change 2022 – Impacts, Adaptation and Vulnerability: Working Group II Contribution to the Sixth Assessment Report of the Intergovernmental Panel on Climate Change*. 1st edn. Cambridge University Press. Available at: https://doi.org/10.1017/9781009325844.

IPCC (2023) *IPCC, 2023: Climate Change 2023: Synthesis Report. Contribution of Working Groups I, II and III to the Sixth Assessment Report of the Intergovernmental Panel on Climate Change [Core Writing Team, H. Lee and J. Romero (eds.)]. IPCC, Geneva, Switzerland.* First. Intergovernmental Panel on Climate Change (IPCC). Available at: https://doi.org/10.59327/IPCC/AR6-9789291691647.

Jacob, D. *et al.* (2020) 'Regional climate downscaling over Europe: perspectives from the EURO-CORDEX community', *Regional Environmental Change*, 20(2), p. 51. Available at: https://doi.org/10.1007/s10113-020-01606-9.

Jehanzaib, M. *et al.* (2022) 'Comprehensive Review: Advancements in Rainfall-Runoff Modelling for Flood Mitigation', *Climate*, 10(10), p. 147. Available at: https://doi.org/10.3390/cli10100147.

Jones, C.N. *et al.* (2019) 'Modeling Connectivity of Non-floodplain Wetlands: Insights, Approaches, and Recommendations', *JAWRA Journal of the American Water Resources Association*, 55(3), pp. 559–577. Available at: https://doi.org/10.1111/1752-1688.12735.

Jonstrup, A. (2024) *Länsstyrelsernas våtmarksarbete - Redovisning av uppdrag A7. Våtmarker i länsstyrelsernas regleringsbrev 2023*. Länsstyrelsen i Gotlands län, p. 26. Available at: https://www.lansstyrelsen.se/download/18.1a5c458718df2882958502c3/1710411839704/L%C3%A4nsstyrelsernas%20v%C3%A5tmarksrapport%202023.pdf.

Kadykalo, A.N. and Findlay, C.S. (2016) 'The flow regulation services of wetlands', *Ecosystem Services*, 20, pp. 91–103. Available at: https://doi.org/10.1016/j.ecoser.2016.06.005.

Karimi, S., Seibert, J. and Laudon, H. (2022) ‘Evaluating the effects of alternative model structures on dynamic storage simulation in heterogeneous boreal catchments’, *Hydrology Research*, 53(4), pp. 562–583. Available at: https://doi.org/10.2166/nh.2022.121.

Laguna Marín, C. (2022) *Assessment of future climate and land use changes on streamflow and phosphorus transport in a Swedish agricultural catchment*. M. Sc. Swedish University of Agricultural Sciences.

Lamontagne, J.R., Barber, C.A. and Vogel, R.M. (2020) ‘Improved Estimators of Model Performance Efficiency for Skewed Hydrologic Data’, *Water Resources Research*, 56(9), p. e2020WR027101. Available at: https://doi.org/10.1029/2020WR027101.

Ledesma, J.L.J. and Futter, M.N. (2017) ‘Gridded climate data products are an alternative to instrumental measurements as inputs to rainfall–runoff models’, *Hydrological Processes*, 31(18), pp. 3283–3293. Available at: https://doi.org/10.1002/hyp.11269.

Ledesma, J.L.J. and Futter, M.N. (2020) ‘Manual - Precipitation, Evapotranspiration and Runoff Simulator for Solute Transport (PERSiST). Parameter description and Calibration strategy.’

Lindau, G. (2021) – *djupmätning av 10 anlagda våtmarker i Mälardalen*. Bachelor of Science. Swedish University of Agricultural Sciences.

Longo-Minnolo, G. *et al.* (2022) ‘Assessing the use of ERA5-Land reanalysis and spatial interpolation methods for retrieving precipitation estimates at basin scale’, *Atmospheric Research*, 271, p. 106131. Available at: https://doi.org/10.1016/j.atmosres.2022.106131.

Lopez, A. (2019) ‘Complete UERRA regional reanalysis for Europe from 1961 to 2019’. ECMWF. Available at: https://doi.org/10.24381/CDS.DD7C6D66.

Lutton, S., Sheldon, F. and Bunn, S.E. (2010) ‘Morphological characteristics of on-farm water storages and their similarity to natural water bodies in the Border Rivers Catchment, Australia’, *Aquatic Conservation: Marine and Freshwater Ecosystems*, 20(1), pp. 47–57. Available at: https://doi.org/10.1002/aqc.1072.

McLaughlin, D.L. *et al.* (2019) ‘Wetland Connectivity Thresholds and Flow Dynamics From Stage Measurements’, *Water Resources Research*, 55(7), pp. 6018–6032. Available at: https://doi.org/10.1029/2018WR024652.

McLaughlin, D.L., Kaplan, D.A. and Cohen, M.J. (2014) ‘A significant nexus: Geographically isolated wetlands influence landscape hydrology’, *Water Resources Research*, 50(9), pp. 7153–7166. Available at: https://doi.org/10.1002/2013WR015002.

Médus, E. *et al.* (2022) ‘Characteristics of precipitation extremes over the Nordic region: added value of convection-permitting modeling’, *Natural Hazards and Earth System Sciences*, 22(3), pp. 693–711. Available at: https://doi.org/10.5194/nhess-22-693-2022.

Moriasi, D.N. *et al.* (2015) 'Hydrologic and Water Quality Models: Performance Measures and Evaluation Criteria', *Transactions of the ASABE*, 58(6), pp. 1763–1785. Available at: https://doi.org/10.13031/trans.58.10715.

Muñoz-Sabater, J. *et al.* (2021) 'ERA5-Land: a state-of-the-art global reanalysis dataset for land applications', *Earth System Science Data*, 13(9), pp. 4349–4383. Available at: https://doi.org/10.5194/essd-13-4349-2021.

Nakashima, N. *et al.* (2024) 'A data-based approach to determining the optimal water ponding scale and zone for small urban wetland restoration', *Restoration Ecology*, p. e14154. Available at: https://doi.org/10.1111/rec.14154.

Nash, J.E. and Sutcliffe, J.V. (1970) 'River flow forecasting through conceptual models part I — A discussion of principles', *Journal of Hydrology*, 10(3), pp. 282–290. Available at: https://doi.org/10.1016/0022-1694(70)90255-6.

Olsson, J. *et al.* (2013) 'Adaptation to climate change impacts on urban storm water: a case study in Arvika, Sweden', *Climatic Change*, 116(2), pp. 231–247. Available at: https://doi.org/10.1007/s10584-012-0480-y.

Olsson, J. *et al.* (2019) 'Short-duration rainfall extremes in Sweden: a regional analysis', *Hydrology Research*, 50(3), pp. 945–960. Available at: https://doi.org/10.2166/nh.2019.073.

Olsson, J. and Foster, K. (2014) 'Short-term precipitation extremes in regional climate simulations for Sweden', *Hydrology Research*, 45(3), pp. 479–489. Available at: https://doi.org/10.2166/nh.2013.206.

Papa, F. and Frappart, F. (2021) 'Surface Water Storage in Rivers and Wetlands Derived from Satellite Observations: A Review of Current Advances and Future Opportunities for Hydrological Sciences', *Remote Sensing*, 13(20), p. 4162. Available at: https://doi.org/10.3390/rs13204162.

Park, J. *et al.* (2014) 'Stochastic modeling of hydrologic variability of geographically isolated wetlands: Effects of hydro-climatic forcing and wetland bathymetry', *Advances in Water Resources*, 69, pp. 38–48. Available at: https://doi.org/10.1016/j.advwatres.2014.03.007.

Quin, A. and Destouni, G. (2018) 'Large-scale comparison of flow-variability dampening by lakes and wetlands in the landscape', *Land Degradation & Development*, 29(10), pp. 3617–3627. Available at: https://doi.org/10.1002/ldr.3101.

Rajczak, J. and Schär, C. (2017) 'Projections of Future Precipitation Extremes Over Europe: A Multimodel Assessment of Climate Simulations', *Journal of Geophysical Research: Atmospheres*, 122(20). Available at: https://doi.org/10.1002/2017JD027176.

Renard, B. and Lang, M. (2007) 'Use of a Gaussian copula for multivariate extreme value analysis: Some case studies in hydrology', *Advances in Water Resources*, 30(4), pp. 897–912. Available at: https://doi.org/10.1016/j.advwatres.2006.08.001.

Rubel, F. *et al.* (2017) 'The climate of the European Alps: Shift of very high resolution Köppen-Geiger climate zones 1800–2100', *Meteorologische Zeitschrift*, 26(2), pp. 115–125. Available at: https://doi.org/10.1127/metz/2016/0816.

Salmonsson, T. (2013) *Assessing the impacts of climate change on runoff along a climatic gradient of Sweden using PERSiST*. M. Sc. Uppsala University.

Sitterson, J. *et al.* (2018) 'An Overview of Rainfall-Runoff Model Types', in *iEMSs 2018. 9th International Congress on Environmental Modelling and Software "Modelling for Sustainable Food-Energy-Water Systems"*, Fort Collins, CO, USA: U.S. Environmental Protection Agency (EPA).

SMHI (2019) 'Climate extremes for Sweden - State of knowledge and implications for adaptation and mitigation'. Available at: https://doi.org/10.17200/CLIMATE_EXTREMES_SWEDEN.

SMHI (2022) 'Climate indicator - Extreme precipitation'. Available at: https://www.smhi.se/en/climate/climate-indicators/climate-indicators-extreme-precipitation-1.91474.

SMHI (2023) 'About the Scenario Service - Meteorology'. Available at: https://www.smhi.se/en/climate/future-climate/about-the-analysis/about-the-scenario-service-meteorology-1.177519.

SMHI (2024) 'Advanced Climate Change Scenario Service'. Available at: https://www.smhi.se/en/climate/future-climate/advanced-climate-change-scenario-service/met/sverige/medeltemperatur/rcp45/2071-2100/year/anom (Accessed: 20 May 2024).

Strand, J.A. *et al.* (2024) *Anlagda våtmarker som flödesbuffrare Hur skapar vi synergieffekter med biologisk mångfald och pollinering? RAPPORT 7148 | MAJ 2024*. Naturvårdsverket, p. 91. Available at: https://www.naturvardsverket.se/49d27d/globalassets/media/publikationer-pdf/7100/978-91-620-7148-6.pdf.

Strand, J.A. and Weisner, S.E.B. (2013) 'Effects of wetland construction on nitrogen transport and species richness in the agricultural landscape—Experiences from Sweden', *Ecological Engineering*, 56, pp. 14–25. Available at: https://doi.org/10.1016/j.ecoleng.2012.12.087.

Sunyer, M.A. *et al.* (2015) 'Inter-comparison of statistical downscaling methods for projection of extreme precipitation in Europe', *Hydrology and Earth System Sciences*, 19(4), pp. 1827–1847. Available at: https://doi.org/10.5194/hess-19-1827-2015.

Thorslund, J. *et al.* (2017) 'Wetlands as large-scale nature-based solutions: Status and challenges for research, engineering and management', *Ecological Engineering*, 108, pp. 489–497. Available at: https://doi.org/10.1016/j.ecoleng.2017.07.012.

Thorslund, J. *et al.* (2018) 'Solute evidence for hydrological connectivity of geographically isolated wetlands', *Land Degradation & Development*, 29(11), pp. 3954–3962. Available at: https://doi.org/10.1002/ldr.3145.

Vautard, R. *et al.* (2021) 'Evaluation of the Large EURO-CORDEX Regional Climate Model Ensemble', *Journal of Geophysical Research: Atmospheres*, 126(17), p. e2019JD032344. Available at: https://doi.org/10.1029/2019JD032344.

Popular science summary

Everyone has experienced it already. A weather forecast says it is going to rain in five days. But if the day has come there is only blue sky and sunshine. It is even more challenging to try to predict rainfall for the next thirty years. Still scientists try to do that with so called climate models. These models can show what could happen in the future. Supercomputers generate them and need a lot of power and storage to do so.

In past years, heavy rain has become more common around the world, also in Sweden. A lot of rain in a short period of time can cause floods. Floods often have massive negative effects like the loss of harvests, the destruction of buildings and infrastructure and the death of humans. In the future it is projected that there will be even more floods.

It is costly to build measures against them though. Manmade wetlands could be a cheaper nature-based solution. A lot of different types of manmade wetlands exist. They can be ditches and ponds in agricultural landscapes or smaller and bigger lakes in nature reserves. At present, it is uncertain which wetland type is best to prevent floods.

This study looks at ten different wetlands in Mälardalen in Sweden. It tries to find out which type of wetland is best to prevent floods and which factors are responsible for that. This is done for the present climate and possible future climates with a hydrological model. A model is a simpler version of reality because it only includes necessary processes and ignores the rest.

In this case, the model predicts how the water level is going to change. Water level changes can be used to judge how good a wetland can prevent or reduce a flood. Here it was of special interest, how water level changes under future climate, which is predicted to be warmer and with more rain.

The results focus on three wetlands of different types. The three wetlands will not dry out in any of the scenarios. Under warmer and wetter conditions, the water level of the three wetland types behaves like under present conditions. Only with more

extreme rainfall water level changes are visibly different from present climate. The water level changes are most evident in summer and fall.

Different factors can be the reason for this behaviour. Firstly, it matters how big the wetland size is compared to the area it receives water from. The higher this relative are the better the wetland can take a lot of rainfall in. Secondly, the purpose and the design of a wetland play an important role. A ditch for example, is designed to receive excess water from agricultural fields constantly. Therefore, a ditch cannot prevent floods very well. A small lake that is supposed to be home to different animals and plants can be better at avoiding floods. Its design does not allow the water level to rise to fast because this could harm the animals and plants living there. Lastly, interactions with other water sources can also affect the ability to prevent floods. These interactions happen mostly underground and are not well understood until today.

This study shows that the current design of different wetland types will be able to handle warmer and wetter climate conditions. However, the current wetland design will struggle to deal with more extreme rainfall. More knowledge and understanding are needed to adapt the design to more rainfall. Only like this, wetlands can be a good solution to prevent floods under future climate scenarios.

Acknowledgements

My deepest gratitude goes to my supervisor, Emma Lannergård. She helped me successfully navigate through this experience with all its ups and downs. She made it a fun, encouraging and educational journey that taught me much more than just how to work scientifically.

I am also profoundly grateful to Martyn Futter for his insights and support on PERSiST which helped me raise the quality of my work significantly.

Appendix

ParName	ParID	D	MinOfNumericValue	MaxOfNumericValue	xRange	z	p
BoxRelativeAreaIndex(0.1)	66	0.940026929404923	0.899999999999989	0.900000001043822	1.14954118331268E-03	4.88018337718638	2.05835549984312E-21
BoxRelativeAreaIndex(0.2)	95	0.927832048922995	0.999999992155683	1.00000061601613	0.01334442166524	4.81687321962275	7.02694275004988E-21
LandCoverInitialSoilTemperature(0)	24	0.882514244127423	###################	3.40091158652095	1.94465401863024E-02	4.58160421749541	5.85281273646199E-19
c(0)	216	0.85258299252559	0.65	1	0.911406521937354	4.42621505580605	9.61930708410877E-18
f(0)	217	0.74552467208122	0.35	0.45	0.21525964164427	3.87041796161765	9.73688164451496E-14
LandCoverSolarRadiationScalingFactor(0)	22	0.523157596117125	70	95	0.241548286235816	2.71599134488179	3.91524411009134E-07
BoxEvapotranspirationAdjustment(0.1)	76	0.491205013144449	0.3	0.486463	0.253893026071237	2.5501083691886	2.24657125836835E-06
BoxInitialWaterDepth(0.0)	35	0.487509782787718	0	15	0.218372570153459	2.53092444881601	2.73014146554428E-06
BoxInitialWaterDepth(0.1)	64	0.459539648184487	150	200	0.2855583910312	2.38571649606644	1.13841741534186E-05
BoxRetainedWaterDepth(0.1)	70	0.438779815326776	100	120	0.7328974623856	2.27794108234558	3.11084475806455E-05
BoxCharacteristicTimeConstant(0.0)	45	0.428238427079791	0.8	3	0.643924701589595	2.22321508877434	5.09140998527875E-05
BoxCharacteristicTimeConstant(0.1)	74	0.420098147430385	2	7	0.128921460412752	2.18095453624333	7.38757907560898E-05
BoxInitialWaterDepth(0.2)	93	0.408218888758937	80	130	0.78076790836678	2.11928294058128	1.25560811309923E-04
LandCoverMinimumSoilTemperatureForInfiltration(0)	32	0.405384855741457	0.1	0.3	0.124026908964425	2.10456995695319	1.42178192909393E-04
SubcatchmentRainMultiplier(0)	222	0.385476091158216	1	1.5	0.60116236566802	2.00121289457525	3.32222345161284E-04
BoxCharacteristicTimeConstant(0.2)	103	0.341054676259912	5	20	0.482474735504793	1.77059753261425	1.89216944863415E-03
BoxCharacteristicTimeConstant(0.3)	132	0.334157880862997	10	20	0.17564604070563	1.73479257299125	2.43207480431785E-03
BoxDroughtRunoffFraction(0.1)	72	0.278683330637491	0.01	0.0500324	0.211512747793882	1.44679446421495	1.52004240193199E-02
n(0)	218	0.277711836482893	0.01	0.09	0.78751575805152	1.44175091761432	1.56498296060625E-02
SubcatchmentSnowMultiplier(0)	221	0.277223876693036	0.7	1	0.865459170810684	1.43921765693773	1.58799347419769E-02
BoxRetainedWaterDepth(0.5)	186	0.258344943537965	80	150	0.231851134893407	1.34120700119969	0.027386831514083
BoxCharacteristicTimeConstant(0.4)	161	0.240192020131773	1	4.5	0.17157268575058	1.24696545100249	4.46038795088681E-02
BoxEvapotranspirationAdjustment(0.0)	47	0.239940742759748	1	2	0.80856819374014	1.24566093555122	4.48948204253541E-02
LandCoverDegreeDayMeltFactor(0)	12	0.205403764313529	2.5	3	0.93089396039196	1.06636097845511	0.102761884169863

Figure 13. Aby - 1. MC analysis, sensitive parameters with D > 0.2.

ParName	ParID	D	MinOfNumericValue	MaxOfNumericValue	xRange	z	p
BoxRelativeEvapotranspirationIndex(0.0)	49	0.868582074799707	-1.26796143052128E-02	0.226709239701524	5.29865526512729E-02	4.50927486284138	2.18019014742461E-18
c(0)	216	0.623380798168496	0.9	1	0.76063570012928	3.23630367781583	7.99269452303387E-10
f(0)	217	0.522125050545841	0.35	0.38	0.2425808318071	2.71063084767097	4.14978475348511E-07
BoxCharacteristicTimeConstant(0.2)	103	0.48628223378406	7.5	20	0.43528639366692	2.52455158432146	2.91185156117609E-06
BoxRetainedWaterDepth(0.1)	70	0.409042720948837	100	120	0.66394468173315	2.12355989481842	1.21085548018341E-04
BoxDroughtRunoffFraction(0.1)	72	0.369583888633257	0.01	0.0500324	0.316690621170664	1.9187079575749	6.34368556404411E-04
BoxInitialWaterDepth(0.0)	35	0.338231280595963	0	5	0.210788327247174	1.75593977318693	2.09825552185407E-03
BoxCharacteristicTimeConstant(0.3)	132	0.328235327240977	10	20	0.25999996687667	1.70404542433778	3.00480788883417E-03
LandCoverMinimumSoilTemperatureForInfiltrat	32	0.288215620754668	0.1	0.2	0.14315692826494	1.49628168880522	1.13592913335591E-02
LandCoverSolarRadiationScalingFactor(0)	22	0.287903223647411	70	80	0.47680265870553	1.49465986806559	1.14700297808143E-02
BoxEvapotranspirationAdjustment(0.1)	76	0.273071117355623	0.3	0.4	0.13869358852673	1.41765845852122	1.79616418195045E-02
LandCoverSnowMeltTemperature(0)	10	0.272236461129948	-1	0	0.546746265051517	1.41332531091578	1.84077573800391E-02
SubcatchmentSnowThresholdTemperature(0)	220	0.269546580469647	0	1	0.593198517569569	1.3993606993984	0.019912081334642
SubcatchmentSnowMultiplier(0)	221	0.259346258234623	0.7	1	0.80836586607776	1.34640536220947	2.66322154304738E-02
BoxInitialWaterDepth(0.2)	93	0.254773821301024	100	130	0.627322840908867	1.32266739256353	3.02298421840292E-02
BoxCharacteristicTimeConstant(0.4)	161	0.225573220213466	1	4.5	0.323446387629671	1.17107142911431	6.43715464146209E-02
BoxInitialWaterDepth(0.1)	64	0.210171211250563	150	170	0.240809180906299	1.0911113494987	9.23805773012797E-02
LandCoverDegreeDayMeltFactor(0)	12	0.205852517565448	2.5	3	0.30395140400318	1.06869069698973	0.101747923300339

Figure 14. Aby - 2. MC analysis, sensitive parameters with D > 0.2.

ParName	ParID	D	MinOfNumericValue	MaxOfNumericValue	xRange	z	p
SubcatchmentSnowThresholdTemperature(0)	220	0.396324883611579	0	0.55	0.729658216944913	2.05753478806288	2.10316123702558E-04
BoxCharacteristicTimeConstant(0.1)	74	0.371278481701672	2	4	0.23656465555323	1.92750549801218	5.92858449428041E-04
BoxDroughtRunoffFraction(0.1)	72	0.311480527465272	0.01	0.03	0.315970452926885	1.61706228290241	5.35469781504407E-03
SubcatchmentRainMultiplier(0)	222	0.301612534704045	1.2	1.5	0.3212203778413	1.56583224604589	0.007419366120704
BoxCharacteristicTimeConstant(0.3)	132	0.290469719047079	10	16	0.356589104482333	1.50798392059568	1.05880190380894E-02
SubcatchmentSnowMultiplier(0)	221	0.290152853774197	0.8	1	0.78034893220557	1.50633890321463	1.06935448404029E-02
BoxRetainedWaterDepth(0.1)	70	0.264782157646111	110	120	0.6177233341167	1.37462602814805	2.28408346579331E-02
LandCoverSnowMeltTemperature(0)	10	0.247942849909462	-1	-0.1	0.542060496968286	1.28720416061523	0.036376320752536
BoxInitialWaterDepth(0.0)	35	0.242590574675622	0.5	5	0.227997660618496	1.25941763258156	4.19054598322243E-02
BoxCharacteristicTimeConstant(0.0)	45	0.234721966784964	1.4	3	0.352369025608494	1.21856747368888	5.13059529103345E-02

Figure 15. Aby - 3. MC analysis, sensitive parameters with D > 0.2.

ParName	ParID	D	MinOfNumericValue	MaxOfNumericValue	xRange	z	p
LandCoverInitialSoilTemperature(0)	24	0.9370905180884360	-3.936380185187010E-23	9.59457145689134E-21	4.085952499799460E-03	4.86493889296253	2.77049523205846E-21
f(0)	217	0.698231768047553	0.3	0.6	0.262552545677937	3.62489516125481	3.86240967080641E-12
BoxCharacteristicTimeConstant(0.0)	45	0.682378087288472	0.1	1	0.741201616700237	3.54259021137783	1.25677034423754E-11
c(0)	216	0.531622663054157	0.5	1	0.649269721877686	2.75993804221633	2.41954536595662E-07
BoxRetainedWaterDepth(0.3)	128	0.351585435034116	80	120	0.334689074769805	1.82526834289791	1.27704169815123E-03
BoxInitialWaterDepth(0.0)	35	0.34497594599919	0	10	0.204043661843947	1.79095494451436	1.63675569540465E-03
BoxCharacteristicTimeConstant(0.5)	190	0.33258129052717	250	500	0.353693219276752	1.72660764795467	2.57386155548555E-03
BoxRetainedWaterDepth(0.5)	186	0.323890325000868	80	120	0.264344969108967	1.6814881900665	3.50065526455626E-03
BoxInitialWaterDepth(0.3)	122	0.315541103596673	80	120	0.8253450251653	1.63814290891256	4.66800038651024E-03
BoxInitialWaterDepth(0.1)	64	0.290180051852874	100	220	0.760768287146992	1.506480103011460	1.06844504734371E-02
BoxInitialWaterDepth(0.2)	93	0.27169836882228	80	120	0.238105552746347	1.41053178548249	1.87004746037608E-02
SubcatchmentSnowThresholdTemperature(0)	220	0.271417648244459	-2	2	0.545927452166027	1.40907441457676	0.018854793228626
BoxCharacteristicTimeConstant(0.1)	74	0.270006766892656	0.3	0.8	0.161365782126952	1.40174977364906	1.96473572599762E-02
BoxCharacteristicTimeConstant(0.2)	103	0.246484992714657	1.5	3	0.69746538487152	1.27963564292085	3.78172908214373E-02
LandCoverSolarRadiationScalingFactor(0)	22	0.235728424316639	60	90	0.293683340389243	1.22379253391033	5.00135410875716E-02
BoxInitialWaterDepth(0.5)	180	0.233249207582332	80	120	0.70383744287645	1.21092159168864	5.32470299974581E-02
n(0)	218	0.233161461832583	0.01	0.1	0.723357540263955	1.21046605649496	5.33645719878666E-02
LandCoverSnowMeltTemperature(0)	10	0.226700804099389	0	5	0.422779235471938	1.17692532112988	6.26274078896237E-02
BoxRetainedWaterDepth(0.4)	157	0.224242548910109	100	220	0.753654313615992	1.16416320151784	6.64805375036223E-02
BoxDroughtRunoffFraction(0.1)	72	0.216897115766724	0	0.03	0.9227794687079	1.12602912301088	7.91524189616968E-02
SubcatchmentSnowMultiplier(0)	221	0.215857235518992	0.5	1.2	0.137083940951596	1.12063054756533	8.10928960957989E-02

Figure 16. Bru - 1. MC analysis, sensitive parameters with D > 0.2.

ParName	ParID	D	MinOfNumericValue	MaxOfNumericValue	xRange	z	p
SubcatchmentSnowThresholdTemperature(0)	220	0.578957578450642	-2	0.6	0.657388950999662	3.00567894606968	1.42257539910847E-08
BoxCharacteristicTimeConstant(0.5)	190	0.537015579283777	275	500	0.227690303069164	2.78793555943109	1.77344908114488E-07
LandCoverSolarRadiationScalingFactor(0)	22	0.419354307225765	63	90	0.286528045715411	2.1770928632547	7.64046751600565E-05
BoxRetainedWaterDepth(0.5)	186	0.397235926885007	84	120	0.30864642605617	2.0622645017549	2.02277558767688E-04
BoxRetainedWaterDepth(0.4)	157	0.340977086258593	130	220	0.791957478415455	1.77019472135126	1.89757464695885E-03
BoxInitialWaterDepth(0.5)	180	0.315157685961697	95	120	0.76613807811856	1.63615238256678	4.72924672588121E-03
BoxCharacteristicTimeConstant(0.2)	103	0.302003097346853	2	3.5	0.635336430680187	1.56785986595502	0.007325678417221
SubcatchmentSnowMultiplier(0)	221	0.273349093963252	0.55	1.2	0.412925415840669	1.4191015840077	1.78151819660301E-02
LandCoverSnowMeltTemperature(0)	10	0.272184227388103	2	3.8	0.370223443074378	1.41305413757946	1.84359953244523E-02
c(0)	216	0.249076917064075	0.85	1	0.719665152358193	1.29309171075176	3.52878596593308E-02
BoxRetainedWaterDepth(0.1)	70	0.227137802005847	120	220	0.599686821613691	1.17919401136869	6.19619296625152E-02
BoxInitialWaterDepth(0.0)	35	0.222692618495985	1	10	0.463581891307937	1.15611668241695	6.90074671631011E-02
BoxInitialWaterDepth(0.1)	64	0.21762969124843	155	220	0.331389916594708	1.12983231478818	7.78077725637302E-02
BoxInfiltration(0.2)	97	0.216942649040362	60	100	0.68753088433448	1.1262655106272	0.079068305322084
BoxInitialWaterDepth(0.4)	151	0.21024877396881	125	220	0.240731618188053	1.09151401912064	9.22187211982965E-02
LandCoverGrowingDegreeThreshold(0)	18	0.207638891478098	-3	-1	0.835089871870255	1.07796472095783	9.77879381274843E-02
BoxInfiltration(0.3)	126	0.206886563208341	60	100	0.204878142674012	1.07405898187588	9.94408678127573E-02
BoxInfiltration(0.1)	68	0.205194567081523	10	50	0.28500151134985	1.06527492355365	0.103237216229242
BoxInfiltration(0.5)	184	0.204788134701 02	60	100	0.265800100593097	1.06316491533449	0.10416553091169

Figure 17. Bru - 2. MC analysis, sensitive parameters with D > 0.2.

ParName	ParID	D	MinOfNumericValue	MaxOfNumericValue	xRange	z	p
SubcatchmentSnowMultiplier(0)	221	0.480495470473195	0.65	1.1	0.205779039330727	2.49450939591812	3.93675313167947E-06
BoxInitialWaterDepth(0.0)	35	0.408697204487369	2	10	0.375616521002827	2.12176613376854	1.22943820256262E-04
LandCoverSolarRadiationScalingFactor(0)	22	0.363853226400063	65	90	0.224382067717584	1.88895701991994	7.95676989378889E-04
BoxCharacteristicTimeConstant(0.0)	45	0.314147235126482	0.7	1.2	0.62787272532256	1.63090659096738	4.89415944819299E-03
BoxCharacteristicTimeConstant(0.1)	74	0.288036807117942	0.3	0.7	0.31980633013696	1.49535337142381	1.14225603487078E-02
c(0)	216	0.278792609454647	0.9	1	0.57291025651347	1.44736178909712	1.51505904408678E-02
SubcatchmentRainMultiplier(0)	222	0.277136831513746	1	1.5	0.54639258025096	1.43876575878061	1.59212934789861E-02
BoxRetainedWaterDepth(0.5)	186	0.274054649272752	80	100	0.29457280170764	1.42276449959597	0.017448127292433
BoxCharacteristicTimeConstant(0.2)	103	0.260276643868129	2.8	3.5	0.632825663475972	1.35123549245466	2.59471842419002E-02
f(0)	217	0.243551375053145	0.3	0.4	0.7368407818096	1.26440566205658	4.08637625857819E-02
BoxInitialWaterDepth(0.2)	93	0.220827339963234	80	105	0.171329522781864	1.14643302229552	7.21510496805754E-02
BoxRetainedWaterDepth(0.1)	70	0.220524823638062	165	220	0.828367960892964	1.14486249798898	7.26716023526974E-02

Figure 18. Bru - 3. MC analysis, sensitive parameters with D > 0.2.

ParName	ParID	D	MinOfNumericValue	MaxOfNumericValue	xRange	z	p
f(0)	217	0.854294643748594	0.15	0.4	0.106489669976896	4.43510115426212	8.21767380411784E-18
Slope(0)	219	0.812417979481835	9.999999860848460E-04	1.000287238218750E-03	0.011111432282871	4.21769695609088	3.53752121833852E-16
BoxCharacteristicTimeConstant(0.3)	132	0.562497319697106	8	15	0.738967909734	2.92022492487047	3.91671589305596E-08
BoxCharacteristicTimeConstant(0.0)	45	0.492215023109748	1	6	0.590254238796022	2.55535187199608	2.12945095425168E-06
LandCoverMinimumSoilTemperatureForInfiltrat	32	0.384033416331454	0	0.3	0.302241093472467	1.9937231966868	3.52709999421054E-04
BoxRetainedWaterDepth(0.3)	128	0.328677833475631	50	100	0.701226853083474	1.70634271125915	2.95809167656974E-03
SubcatchmentSnowMultiplier(0)	221	0.248920049619677	0.5	1	0.758723971188304	1.29227732781162	3.54367489614519E-02
c(0)	216	0.2488743768532	0.6	0.99	0.28809006312771	1.29204021601325	3.54801990757885E-02
BoxCharacteristicTimeConstant(0.2)	103	0.233327574705219	1	6	0.507837378626788	1.211328437406	5.31422326957357E-02
BoxInitialWaterDepth(0.0)	35	0.219193094810501	0	10	0.231787297346362	1.13794878021783	7.49992370484799E-02
BoxCharacteristicTimeConstant(0.4)	161	0.216922517892641	0.5	2	0.214450031126967	1.12616099905482	7.91054879911182E-02
SubcatchmentSnowThresholdTemperature(0)	220	0.216116473887948	0	2	0.843567454280105	1.12197639281649	8.06056341483254E-02
BoxInfiltration(0.2)	97	0.215231443238576	0	100	0.157317576369267	1.1173817245913	8.22787888019097E-02
BoxRetainedWaterDepth(0.2)	99	0.213241001713388	150	200	0.139700174757 2	1.10704827632441	8.61424957118902E-02

Figure 19. Gra - 1. MC analysis, sensitive parameters with D > 0.2.

ParName	ParID	D	MinOfNumericValue	MaxOfNumericValue	xRange	z	p
f(0)	217	0.504994857867594	0.15	0.18	0.338142397034367	2.62169884057486	1.07133007431446E-06
BoxInitialWaterDepth(0.3)	122	0.311902465336824	55	100	0.354764201329842	1.61925278843214	5.27931284444387E-03
SubcatchmentSnowMultiplier(0)	221	0.300443480713765	0.7	1.3	0.574953284635333	1.55976306050244	7.70626174115396E-03
LandCoverCanopyInterception(0)	20	0.296189682905566	0	0.03	0.252829924937571	1.53767931725625	8.83604363322398E-03
LandCoverMinimumSoilTemperatureForInfiltratior	32	0.286305217899248	0	0.1	0.18428301739487	1.48636376415103	1.20516195068338E-02
BoxCharacteristicTimeConstant(0.0)	45	0.266496099874517	4	6	0.697868648894125	1.38352402044048	2.17468205174385E-02
BoxRetainedWaterDepth(0.4)	157	0.248137846190486	100	170	0.620686865798329	1.28821649077248	3.61871625211621E-02
LandCoverSolarRadiationScalingFactor(0)	22	0.217000276552975	50	80	0.609157139298073	1.12656468591711	7.89619522900339E-02
BoxRetainedWaterDepth(0.3)	128	0.208074469874511	65	100	0.698270548305883	1.08022604175954	9.68407231132106E-02
LandCoverDegreeDayMeltFactor(0)	12	0.200644632460122	2	4	0.671232867754 24	1.04165377546516	0.113998002266588

Figure 20. Gra - 2. MC analysis, sensitive parameters with D > 0.2.

ParName	ParID	D	MinOfNumericValue	MaxOfNumericValue	xRange	z	p
c(0)	216	0.348083492530587	0.7	0.85	0.573485134920394	1.80708788331852	1.45735338370737E-03
LandCoverCanopyInterception(0)	20	0.313942939028721	0	0.02	0.52919431587324	1.62984598047939	4.92812858746141E-03
BoxRelativeEvapotranspirationIndex(0.1)	78	0.271488548691685	0.25	0.8	0.702861097711293	1.40944249678075	1.88157129133235E-02
BoxCharacteristicTimeConstant(0.0)	45	0.259943421888717	4.5	6	0.71092381404558	1.34950555864748	2.61907633966822E-02
BoxInitialWaterDepth(0.0)	35	0.237574337431321	5	10	0.174190368451032	1.23337565777222	4.77135577665577E-02
SubcatchmentRainMultiplier(0)	222	0.231909387899361	0.7	1.2	0.6112278670026	1.20396586995266	5.50653455368359E-02
BoxCharacteristicTimeConstant(0.3)	132	0.223442186132992	12	15	0.3451852648474	1.16000808957538	6.77758590892077E-02
f(0)	217	0.204961921905317	0.15	0.16	0.2656263133888	1.06406713781243	0.103767809581259
SubcatchmentSnowThresholdTemperature(0)	220	0.204657605742865	0.6	2.3	0.616422311625218	1.06248726958637	0.104465022301905

Figure 21. Gra - 3. MC analysis, sensitive parameters with D > 0.2.

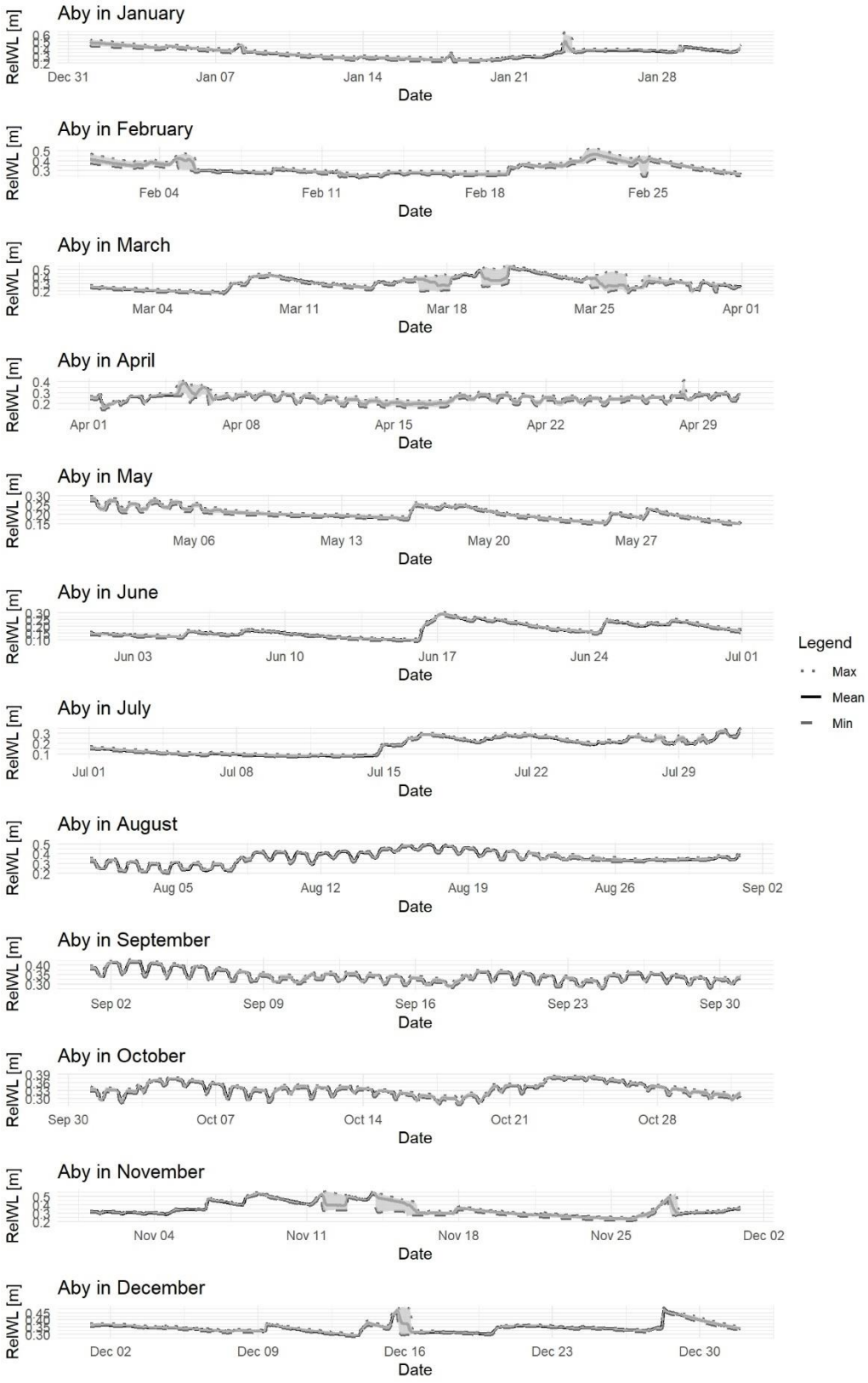

Figure 22. Minimum, mean and maximum relative water level changes for each month for 2041 in Aby.

	R2	N-S	Log(N-S)	RMSE	RE	AD	V.
Reach flow	-999	-999	-999	-999	-999	-999	-9
Reach depth	0.57542	0.56139	0.57138	0.067252	-47.832	-0.0087875	2.
Reach velocity	-999	-999	-999	-999	-999	-999	-9
SMD	-999	-999	-999	-999	-999	-999	-9
Soil temperature	-999	-999	-999	-999	-999	-999	-9

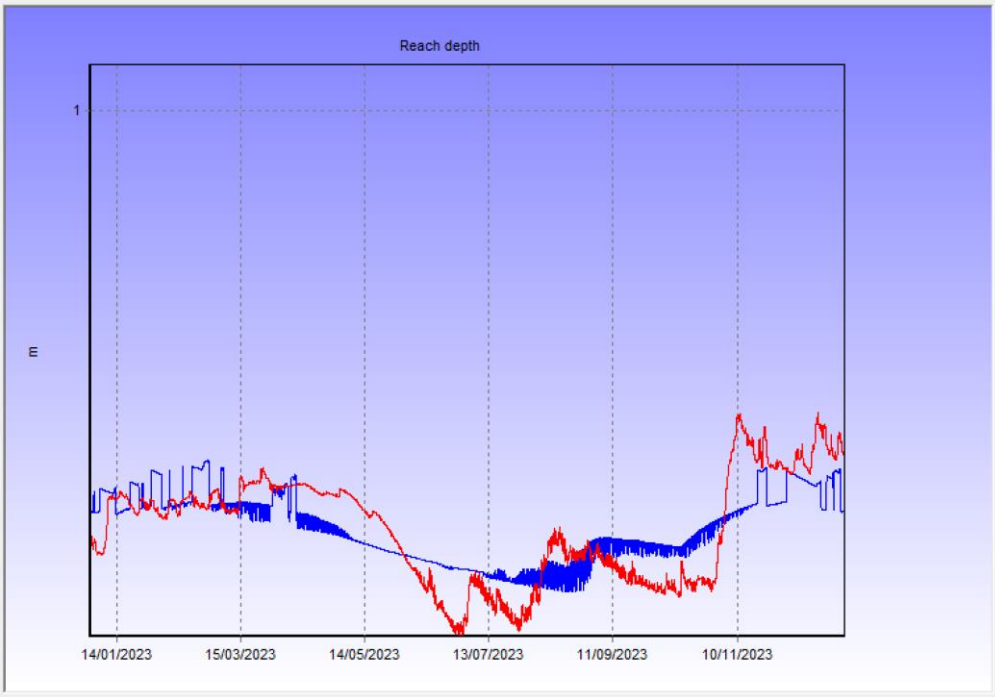

Figure 23. High NSE (0.56139) with poor visual accordance after initial manual calibration.

Publishing and archiving

Approved students' theses at SLU are published electronically. As a student, you have the copyright to your own work and need to approve the electronic publishing. If you check the box for **YES**, the full text (pdf file) and metadata will be visible and searchable online. If you check the box for **NO**, only the metadata and the abstract will be visible and searchable online. Nevertheless, when the document is uploaded it will still be archived as a digital file. If you are more than one author, the checked box will be applied to all authors. You will find a link to SLU's publishing agreement here:

- https://libanswers.slu.se/en/faq/228318.

☒YES, I/we hereby give permission to publish the present thesis in accordance with the SLU agreement regarding the transfer of the right to publish a work.

☐ NO, I/we do not give permission to publish the present work. The work will still be archived and its metadata and abstract will be visible and searchable.